Copy 5
RM L52E29

NACA RM L52E29

NACA FOR REFERENCE

NOT TO BE TAKEN FROM THIS ROOM

RESEARCH MEMORANDUM

A CORRELATION WITH FLIGHT TESTS OF RESULTS OBTAINED FROM THE MEASUREMENT OF WING PRESSURE DISTRIBUTIONS ON A $\frac{1}{4}$-SCALE MODEL OF THE X-1 AIRPLANE (10-PERCENT-THICK WING)

By Jack F. Runckel and James H. Henderson

Langley Aeronautical Laboratory
Langley Field, Va.

CLASSIFICATION CANCELLED

Authority NACA Res. Ab+ Date 5/14/56
RN 161
By MSA 6/5/56 See

CLASSIFIED DOCUMENT

This material contains information affecting the National Defense of the United States within the meaning of the espionage laws, Title 18, U.S.C., Secs. 793 and 794, the transmission or revelation of which in any manner to an unauthorized person is prohibited by law.

NATIONAL ADVISORY COMMITTEE
FOR AERONAUTICS

WASHINGTON

September 3, 1952

NASA Technical Library
3 1176 01436 4765

NATIONAL ADVISORY COMMITTEE FOR AERONAUTICS

RESEARCH MEMORANDUM

A CORRELATION WITH FLIGHT TESTS OF RESULTS OBTAINED FROM THE MEASUREMENT OF WING PRESSURE DISTRIBUTIONS ON A $\frac{1}{4}$-SCALE MODEL OF THE X-1 AIRPLANE (10-PERCENT-THICK WING)

By Jack F. Runckel and James H. Henderson

SUMMARY

An investigation was made in the Langley 16-foot transonic tunnel of the aerodynamic characteristics of a $\frac{1}{4}$-scale model of an X-1 airplane in order to correlate wing pressure-distribution results obtained in a slotted wind tunnel with flight test data on the full-scale airplane. Results were obtained through a Mach number range from 0.70 to 1.00 at Reynolds numbers up to 4.6 million and at angles of attack up to 15° at lower speeds and up to 5° at a Mach number of 1.00.

Evidence was not found to indicate that restrictions or interference effects of sufficient magnitude existed to affect the validity of wing pressure data obtained with the relatively large model that was tested in the slotted 16-foot wind tunnel.

The results indicate that chordwise pressure distributions and spanwise-loadings derived from the two techniques are in good agreement. The wing-panel pitching moments obtained in the wind tunnel were more negative than those shown in the flight results because of some differences in the two airfoil contours near the trailing edges, but the static longitudinal stability of the wing was about the same.

Midsemispan section data obtained in the slotted tunnel was found to be in good agreement with two-dimensional data.

INTRODUCTION

The aerodynamic characteristics of a $\frac{1}{4}$-scale model of the X-1 airplane were determined in the Langley 16-foot transonic tunnel in order to

investigate the validity of aerodynamic data obtained with a relatively large model in a slotted transonic test section by comparing the results with similar data obtained in flight on the full-sized airplane. The model used for this investigation was the X-1 airplane number 2, which has a 10-percent-thick wing. (For convenience, the model is designated hereinafter as the X-1-2 airplane.) A correlation with flight tests based on wing-pressure-distribution comparisons was selected, because this wind-tunnel technique was thought to be free of wind-tunnel interference effects and the NACA Muroc Flight Station was already in the process of accumulating wing-pressure-distribution data on the X-1-2 airplane. The available published data on the X-1-2 wing-pressure-distribution measurements are given in references 1 to 5.

The present investigation reports the results of pressure-distribution measurements obtained in the Langley 16-foot transonic tunnel through a Mach number range from 0.7 to 1.0 at Reynolds numbers up to 4.6 million and through an angle-of-attack range up to 15° at lower speeds and up to 5° at the highest speed. These data are compared with results obtained from the full-scale airplane wing.

SYMBOLS

M	Mach number
R	Reynolds number; based on a wing mean aerodynamic chord of 1.203 ft
p	static pressure in undisturbed stream, lb/sq ft
p_u	local static pressure on upper surface, lb/sq ft
p_l	local static pressure on lower surface, lb/sq ft
q	incompressible dynamic pressure, lb/sq ft
P	pressure coefficient, $\frac{p_u - p}{q}$ or $\frac{p_l - p}{q}$
P_R	resultant pressure coefficient, $\frac{p_l - p_u}{q}$
P_{cr}	pressure coefficient for local sonic velocity
S	area of wing panels outboard of station A (fig. 1); 6.211 sq ft
b	twice spanwise distance from station A to tip; 5.708 ft

c local wing chord parallel to plane of symmetry, ft

$\bar{c}$ average chord of test panel, S/b, ft

c' mean aerodynamic chord of test panel from station A to tip, $\frac{2}{S}\int_0^{b/2} c^2 dy$; 1.119 ft

x chordwise distance from leading edge of local chord, ft

y spanwise distance outboard of station A (fig. 1), ft

c_n section normal-force coefficient, $\int_0^1 (p_l - p_u)\, d\frac{x}{c}$

$c_{m_{c/4}}$ section pitching moment about 0.25 local chord, $\int_0^1 (p_u - p_l)\left(\frac{x}{c} - 0.25\right) d\frac{x}{c}$

c_m section pitching-moment coefficient about a line perpendicular to plane of symmetry, passing through 0.25-chord point of mean aerodynamic chord of test panel, $\int_0^1 (p_u - p_l)\left(\frac{x}{c} - \frac{0.40c - 0.15c'}{c}\right) d\frac{x}{c}$

C_N wing-panel normal-force coefficient, $\int_0^1 c_n \frac{c}{\bar{c}}\, d\frac{2y}{b}$

C_B wing-panel bending-moment coefficient about station A, $\int_0^1 c_n \frac{c}{\bar{c}} \frac{2y}{b}\, d\frac{2y}{b}$

C_m wing-panel pitching-moment coefficient about 0.25 panel mean aerodynamic chord, $\frac{\bar{c}}{c'}\int_0^1 c_m \left(\frac{c}{\bar{c}}\right)^2 d\frac{2y}{b}$

$(C_{m_o})_w$ pitching-moment coefficient of wing panel at zero normal force $(C_m$ at $C_N = 0)$

x_{cp}/c' wing-panel center of pressure position along panel mean aerodynamic chord

$y_{cp}/b/2$ wing-panel lateral center of pressure position

α angle of attack of fuselage center line, deg

α_l section geometric angle of attack, deg

δ_{a_L} flight value of left aileron deflection, deg

Subscript:

A airplane

MODEL AND APPARATUS

The model tested in this investigation was a $\frac{1}{4}$-scale model of the X-1-2 airplane having a 10-percent-thick steel wing, magnesium fuselage, and an aluminum-alloy empennage with an 8-percent-thick horizontal tail. Figure 1 shows the principal dimensions of the model as tested in the Langley 16-foot transonic tunnel and photographs of the model and sting-support system are shown in figure 2.

The model wing, which did not have ailerons, incorporated an NACA 65-110 (a = 1) airfoil section which differed slightly from the actual airplane wing in that the airfoil sections of the full-size airplane were modified over the landing flaps and the ailerons were uncusped (fig. 1(c)). The 0.40-chord line of the wing was unswept (fig. 1(a)). The wing had an incidence angle of 2.5° with respect to the fuselage axis at the fuselage center line and 1.5° at the wing tip, an aspect ratio of 6, a taper ratio of 0.50, and a total wing area including that enclosed by the fuselage of 8.116 square feet.

Pressure-distribution measurements were obtained over six spanwise stations on the left wing. Each spanwise station had 22 orifices on both the upper and lower surfaces and a leading-edge orifice. Figure 1(b) presents the spanwise and chordwise location of the measuring orifices. A nose-boom pitot-static tube was used to check the free-stream Mach number at low angles of attack.

Pressures were recorded by photographing mercury manometer boards. An electrical integrator for wing pressures was coupled to the pressure

transmitting system and was used in determining section normal-force and pitching-moment coefficients. (See ref. 6.)

The Langley 16-foot transonic tunnel in which this investigation was conducted has a slotted test section which permits a continuous variation in speed to Mach numbers slightly above 1.0. A description of the tunnel is presented in reference 7.

TESTS AND ACCURACY OF MEASUREMENTS

Tests

The tests were made for a Mach number range from about 0.7 to 1.0. The Reynolds number and Mach number field for these tests is presented in figure 3. The angle-of-attack range was limited at high angles by loads imposed on the sting support system and varied from about -4° to 15° at $M = 0.70$ and from -2° to 5° at the maximum Mach number for this investigation.

Accuracy of Measurements

The average error in pressure coefficients was found to be about ± 0.002 for the Mach number range tested. The average difference obtained by the electrical integrator and by manual integration was within ± 0.02 for the section normal-force coefficient and ± 0.002 for the pitching-moment coefficient.

The Mach number over the test region is believed to be accurate to ± 0.005. (See ref. 7.) Measurements from the nose-boom pitot-static tube showed excellent agreement with tunnel calibration data over the Mach number range at low angles of attack. This check and the general agreement of the data with flight results indicate that the Mach number measurements in the two cases are correct.

The angle of attack of the model was derived from the sting angle and a correction was obtained by determining the deflection of the model under applied normal load and pitching moments. The angle measurements uncorrected for air stream angularity are believed to be accurate to within $\pm 0.05^\circ$. The upflow angle of the tunnel air stream (ref. 7) was derived from point measurements at the tunnel center line. Since further surveys were not made covering the flow field occupied by a large model such as the present X-1-2 configuration, a stream-angle correction has not been applied to the data reported herein.

Factors Influencing the Correlation Results

In order to correlate the results of the wind-tunnel investigation with pressure-distribution measurements obtained on the wing in flight, the effects of the physical differences between the model and the airplane on the accuracy of the correlation must be considered. The differences between the model airfoil contour near the trailing edge and the control surfaces of the airplane previously mentioned, together with the small aileron deflections occurring during the flight tests, may cause some differences in the loadings over the rear 15 percent of the airfoils. The aileron deflections noted in the selected flight data were all less than 1° and since the aileron is sealed, it is believed that these small deflections would have a negligible effect on the pressure distribution. Some difficulties in correlating the data obtained from the two test facilities were due to the available instrumentation in each case. The orifice locations on the model wing closely conforms with those of the airplane but additional orifices were placed at the 7.5-, 15-, and 25-percent chord stations and none of the 97.5-percent chord on the upper surface. Throughout the tunnel tests only a few orifices produced unusable data (figs. 4, 5, and 6), whereas data are unavailable for several orifices at each span station for the flight data. This lack of data somewhat limits the comparisons because of the inability to define accurately the shock position and determine at what point the deflections in the pressure diagrams occur. Aeroelastic wing bending was considered to be negligible because both unswept wings were of rigid construction. The rear 16.7 percent of the model fuselage length was modified from the clover leaf section used on the airplane to an oval section in order to permit the use of a sting of sufficient strength to support the forces on the model. It was assumed that the wing pressures would not be affected by this modification. A further cause for some disagreement in the correlation comes about from comparing steady-state wind-tunnel data to the high rate of change of angle-of-attack data that occurs in flight during a pull-up.

RESULTS AND DISCUSSION

The results of the tests of the $\frac{1}{4}$-scale model of the X-1-2 airplane in the Langley 16-foot transonic tunnel are presented in the following figures:

Basic Pressure Measurements

Section characteristics . . . . . Figures 4 to 9
Panel characteristics . . . . . Figures 10 to 13 and table I

Correlation With Flight Measurements

Basic Pressure Measurements

Section characteristics.- The chordwise pressure distributions presented in figures 4, 5, and 6 illustrate the variations in the upper and lower surface pressure coefficients at six spanwise stations on the left wing for angles of attack of approximately 0°, 2.5°, and 5°. Included in the figures are values of the integrated section normal-force and pitching-moment coefficients and the wing-panel normal-force coefficient.

The chordwise pressure distributions at a Mach number of approximately 0.85 given in figure 4 show that the position of the shocks on the upper and lower surfaces is approximately the same at all spanwise stations and is comparatively insensitive to the angle of attack from a range of 0° to 5°. At the lowest angle of attack, pressure recovery over the rear portion of the airfoil is indicated and, at 4.9°, separation is evident. The distributions are quite similar spanwise, although the inboard station A shows the greater tendency to produce peak pressures near the leading edge. This result can be attributed to higher incidence at the root station and to fuselage interference effects. The maximum section normal-force coefficient usually occurs near the midsemispan.

The chordwise pressure distributions at a high subsonic speed presented in figure 5 ($M \approx 0.95$) show that the shocks have moved back near the trailing edge of the airfoil. Higher positive pressures are reached on the rear portion of the lower surface of the airfoil so that the loading in this region is increased. This effect is most pronounced at the inboard and outboard sections. The maximum section normal-force coefficient has moved inboard to station B.

The pressure distributions at a Mach number of 1.00 are similar to those for $M \approx 0.95$. As the normal-force coefficient increases, the pressure coefficients on the upper surface approach a constant value across the chord.

The increase in loading at the rear portion of the airfoil exhibited at the transonic speeds in figures 5 and 6 is believed to be characteristic of cusped sections. This tendency is evident in data on the X-1-1 airplane with the NACA 65-108 section from flight tests (ref. 8) and in other test facilities (ref. 9).

The section normal-force coefficients obtained from the integrated pressure distributions are shown plotted against the section local geometric angle of attack in figure 7. These plots show how the section normal-force curves vary spanwise as indicated by the data for stations A, C, E, and F. The earlier stall for the inboard station A which is evident at $M = 0.70$ and 0.80 is probably due to interference effects. At a Mach number of 0.80, a sharp stall occurs at $\alpha_l = 10^\circ$ at the inboard station. At a Mach number of 0.90, all stations exhibit a concave nonlinearity in the low angle-of-attack range which tends to decrease near sonic speeds. In general, subsonically, station C has the highest lift-curve slope with the slope decreasing outboard. Stations C and D should most nearly approach two-dimensional conditions of all the stations shown.

A comparison of pressures at station C near midspan with unpublished two-dimensional data from the Langley 4- by 19-inch high-speed tunnel is presented in figure 8. The actual angle and Mach number of the two-dimensional data may be somewhat different as only approximate adjustment for Mach number and deflection of the tunnel jet have been applied. The agreement with the two-dimensional data is good in spite of the fact that the angle of attack of the two-dimensional tests may be somewhat in error. The angles of attack for the data of the Langley 16-foot transonic tunnel may also be in error since the stream angularity at this spanwise station is unknown but the error is believed to be less than 0.25°.

A comparison of the section normal-force coefficients against the section local angle of attack for a midspan station D with two-dimensional data at several Mach numbers is presented in figure 9. The slopes of the curves are approximately the same except for negative angles of attack at Mach numbers of 0.70, 0.80, and 0.90. At a Mach number of 0.70, the curves are in good agreement up to the force break where a sharp stall occurs in the two-dimensional data. At a Mach number of 0.80, both curves break at approximately the same position with the two-dimensional data having the sharper break. At $M = 0.90$, both curves show a concave nonlinearity in the low angle range, whereas at $M = 1.0$, both curves are linear. In general, the slopes and trends of the curves are in good agreement.

Panel characteristics.- The wing has been treated as an isolated panel and the coefficients obtained from the pressure distributions are based on the geometric properties of the wing panel outboard of station A. (See fig. 1(b).) The variations of panel span-load distributions with normal-force coefficient shown in figure 9 for Mach numbers of 0.85, 0.95, and 1.00 were obtained from cross-faired data. At $M = 0.85$ (fig. 10(a)), theoretical spanwise loading distributions obtained from reference 10 are compared with the experimental data, although this speed

is above the critical Mach number for these airfoil sections. The experimental results differ from the theoretical elliptical distributions in that the test results indicate unloading near midspan and higher loading of the tip sections for the same normal-force coefficient. At $M = 0.95$ (fig. 10(b)), the loadings are similar to $M = 0.85$, but the spanwise irregularities are less severe. At $M = 1.00$ (fig. 10(c)), the loading distribution approaches the elliptical type and resembles that normally found for straight wings at low subsonic speeds.

The spanwise variations of section pitching-moment parameter with panel normal-force coefficient given in figure 11(a) show that, as the normal-force coefficient increases, the pitching-moment parameter increases positively over the inboard portion of the wing. This increase results from the tendency of the upper-surface pressures to peak on the forward portion of the wing at the inboard station. (See figs. 4 to 6.) The distributions at $M = 0.95$ and 1.00 (figs. 11(b) and (c)) are, however, more uniform as were the normal-load distributions.

The variation of wing-panel pitching-moment coefficient with wing panel normal-force coefficient presented in figure 12 shows the wing to be unstable at the lowest test speed ($M = 0.70$) but becoming more stable at the higher test speeds, the greatest increase in stability occurring at about 0.90. At a Mach number of 0.90, however, the wing becomes unstable at about zero normal-force coefficient. This phenomenon has also been noticed for the NACA 65-108 wing as indicated in reference 11.

Figure 13 presents plots of aerodynamic-center position and the pitching-moment coefficient of the wing panel at zero lift as a function of the Mach number. The aerodynamic-center position moves rearward as the speed increases up to a Mach number of about 0.95, above which the aerodynamic center of the wing panel tends to move slightly forward. The aerodynamic center positions represent average values obtained from the portions of the wing-panel lift and moment curves lying below the force breaks. The zero-lift pitching moment of the wing panel becomes more negative up to a Mach number of 0.85 and then becomes rapidly more positive until a Mach number of 0.90 is reached where again there is a reversal until for $M = 0.95$ to $M = 1.00$ the zero-lift pitching-moment coefficient remains fairly constant at about -0.022.

The integrated values of section and panel aerodynamic characteristics are summarized in table I. The Mach numbers listed in table I have been calculated to three decimal places in order to be comparable with flight information. Bending-moment coefficients for the wing panel have been included to permit correlation with tabulated flight values. (See refs. 2 to 5.)

Correlation of Pressure Measurements

Section characteristics.- In order to correlate the results of the wind-tunnel investigation with flight-wing pressure-distribution measurements, comparisons on the basis of chordwise loadings are presented in figures 14 and 15.

Figure 14(a) represents a comparison of wind-tunnel and flight data at about $M = 0.75$. The flight data have been obtained from reference 3 which presents resultant pressure coefficients for stations A, B, C, E, and F and upper and lower surface pressure coefficients for station D. In general, the data from both facilities are in good agreement, although the position of the shock on the upper surface (station D) is farther forward for the flight data than is indicated from wind-tunnel results. The agreement between the two sets of data is much better at the outboard stations E and F. Small differences in Mach number and angle of attack may cause appreciable changes in the shock position. However, in spite of these small differences, the agreement of the data in general is very good.

Figure 14(b) presents a correlation at approximately $M = 0.80$ with flight data obtained from reference 4. The agreement is excellent although a higher peak pressure coefficient is realized at the point where shock occurs at the midspan station D on the flight data.

Figures 14(c) and (d) represent pressure distributions obtained from cross plots of wind-tunnel data at $M = 0.942$ which are compared with flight results presented in reference 3 representing a pull-up at $M \approx 0.95$. Again the agreement is very good for all stations except near the trailing edges where some differences occur. The increased loading at the trailing edge of the wind-tunnel data is due to the airfoil cusp. In addition, some differences of the flight pressure distribution over the rear 15-percent chord for stations D, E, and F may be due to the small aileron deflections which were present.

A comparison of flight and wind-tunnel data at sonic speeds is presented in figures 14(e) and (f). At the higher loading (fig. 14(f)), the agreement with the flight data obtained from reference 5 is good.

Inasmuch as the chordwise loading comparisons do not bring out spanwise differences occurring on both surfaces of the wing, additional comparisons of the upper- and lower-surface pressure distributions at stations A, C, and F obtained from the wind-tunnel test data and unpublished flight data are presented in figure 15 for speeds near a Mach number of 1.0. The agreement on both the upper and lower surface is very good in figure 15(a) except for the expected differences near the trailing edge.

The variation of section pitching-moment coefficient about the quarter-chord point with section normal-force coefficient for several stations are compared with corresponding flight data in figure 16. As would be expected from the differences in loading near the trailing edges, the wind-tunnel data indicate greater negative values of pitching-moment coefficient for corresponding normal-force coefficients. At the highest speed, the agreement is better since the shock has moved to the rear of the airfoil in both cases and the rear portion of the airfoils have separated flow. At lower speeds, slight differences in the shock positions can affect the section coefficients greatly and the accuracy of the pressure-distribution diagrams are affected by the available instrumentation and constancy of test conditions. These flight data were obtained from references 1, 4, and unpublished data. Included in figure 16(c) is the variation of center-of-pressure position at station D with section normal-force coefficient.

The manner in which the section pitching-moment coefficient and center-of-pressure position for station D vary with Mach number is illustrated in figure 17 for tunnel and flight data. At the higher speeds, as also indicated in figure 16, the agreement is very good.

Panel characteristics.- A comparison of the spanwise loading distribution obtained in the wind tunnel with those obtained in flight is given in figure 18. The agreement is very good for all cases. Similar comparisons are shown in figure 19 for the spanwise pitching-moment distribution. The agreement here is much poorer than for the normal loadings as would be expected from inspection of the data of figure 16. In general, the tunnel pitching-moment data are more negative than the flight values.

The wing stability as indicated by the panel coefficients obtained in the tunnel and flight is shown in figure 20. This figure shows the same trends in agreement as were shown in figure 16 for the section coefficients. Prediction of airplane wing pitching-moment coefficients through the use of wind-tunnel data for the reflexed airfoil may involve appreciable error amounting to as much as 0.05 at a Mach number of 0.85.

Chordwise and spanwise center-of-pressure travel with Mach number for the wing panel is shown for a panel normal-force coefficient of about 0.35 for both tunnel and flight data. (See fig. 21.) The chordwise center-of-pressure position along the mean aerodynamic chord is seen to be in agreement at Mach numbers above 0.90. The center-of-pressure position for the tunnel model along the mean aerodynamic chord was 31 percent at $M = 0.70$, increased to 44 percent at $M = 0.85$, and then shifted forward to 23 percent at $M = 0.90$ with a return to a more rearward position of about 45 percent above $M = 0.95$. Above this Mach number the shocks remain at the trailing edge of the airfoil. The

flight center-of-pressure position was a maximum of about 5 percent farther forward at $M = 0.85$. The spanwise center-of-pressure positions are in good agreement throughout the Mach number range.

The general good agreement between the flight and wind-tunnel results serves as evidence that there is negligible effect of restrictions and tunnel-wall interference on pressure data obtained from a sting-supported model of this size or smaller in the Langley 16-foot slotted wind tunnel at high subsonic and transonic speeds. The spanwise loading comparisons offer ample evidence that the corrections which are a function of the lift coefficient are negligibly small and need not be applied to the slotted-tunnel data for these tests. Furthermore, in spite of the flight Reynolds numbers being about three times as large as those for the wind tunnel, the good agreement of the correlation data indicates negligible scale effect for these tests run at a Reynolds number of about 4.5 million.

CONCLUSIONS

An investigation was made in the Langley 16-foot transonic tunnel of the aerodynamic characteristics of a $\frac{1}{4}$-scale model of the X-1-2 airplane in order to correlate wing pressure distribution results obtained in a slotted wind tunnel at transonic speeds with flight test data on the full-scale airplane. A comparison of data obtained in the wind tunnel with that obtained in flight leads to the following conclusions:

1. Evidence was not found to indicate that restrictions or interference effects of sufficient magnitude existed to affect the validity of wing pressure distribution data obtained with the relatively large model that was tested in the Langley 16-foot slotted wind tunnel.

2. Chordwise pressure distributions and spanwise loadings are in good agreement with those obtained in flight on the X-1-2 airplane.

3. A comparison of the chordwise center-of-pressure positions shows good agreement above a Mach number of 0.90. Below this speed the center of pressure from the flight tests was about five percent farther forward on the mean aerodynamic chord. The spanwise center-of-pressure positions were in agreement throughout the Mach number range.

4. The wind-tunnel pitching-moment coefficients were greater negatively than those obtained in flight because of slight differences in trailing-edge contours of the airfoils, but the static stability of the

wing was about the same. The wing-panel pitching-moment coefficient variation with normal-force coefficient obtained in the wind tunnel showed a decrease in stability near zero lift at a Mach number of 0.90.

5. It was found that the midsemispan section data of the model wing obtained in the slotted tunnel were in good agreement with two-dimensional data.

Langley Aeronautical Laboratory
National Advisory Committee for Aeronautics
Langley Field, Va.

REFERENCES

1. Carner, H. Arthur, and Knapp, Ronald J.: Flight Measurements of the Pressure Distribution on the Wing of the X-1 Airplane (10-Percent-Thick Wing) over a Chordwise Station near the Midspan, in Level Flight at Mach Numbers from 0.79 to 1.00 and in a Pull-Up at a Mach Number of 0.96. NACA RM L50H04, 1950.

2. Knapp, Ronald J.: Tabulated Pressure Coefficients and Aerodynamic Characteristics Measured on the Wing of the Bell X-1 Airplane in an Unaccelerated Low-Speed Stall, in Push-Overs at Mach Numbers of 0.83 and 0.99, and in a Pull-Up at a Mach Number of 1.16. NACA RM L51F25, 1951.

3. Smith, Lawrence A.: Tabulated Pressure Coefficients and Aerodynamic Characteristics Measured on the Wing of the Bell X-1 Airplane in an Unaccelerated Stall and in Pull-Ups at Mach Numbers of 0.74, 0.75, 0.94, and 0.97. NACA RM L51B23, 1951.

4. Carner, H. Arthur, and Payne, Mary M.: Tabulated Pressure Coefficients and Aerodynamic Characteristics Measured on the Wing of the Bell X-1 Airplane in Level Flight at Mach Numbers from 0.79 to 1.00 and in a Pull-Up at a Mach Number of 0.96. NACA RM L50H25, 1950.

5. Knapp, Ronald J., and Wilken, Gertrude V.: Tabulated Pressure Coefficients and Aerodynamic Characteristics Measured on the Wing of the Bell X-1 Airplane in Pull-Ups at Mach Numbers from 0.53 to 0.99. NACA RM L50H28, 1950.

6. Helfer, Arleigh P.: Electrical Pressure Integrator. NACA TN 2607, 1952.

7. Ward, Vernon G., Whitcomb, Charles F., and Pearson, Merwin D.: Air-Flow and Power Characteristics of the Langley 16-Foot Transonic Tunnel With Slotted Test Section. NACA RM L52E01, 1952.

8. Beeler, De E., McLaughlin, Milton D., and Clift, Dorothy C.: Measurements of the Chordwise Pressure Distributions over the Wing of the XS-1 Research Airplane in Flight. NACA RM L8G21, 1948.

9. Habel, Louis W., and Henderson, James H.: Preliminary Investigation of Airfoil Characteristics in the Langley Annular Transonic Tunnel. NACA RM L50E18, 1950.

10. DeYoung, John, and Harper, Charles W.: Theoretical Symmetric Span Loading at Subsonic Speeds for Wings Having Arbitrary Plan Form. NACA Rep. 921, 1948.

11. Turner, Thomas R.: Maximum-Lift Investigation of a $\frac{1}{40}$-Scale X-1 Airplane Wing at Mach Numbers from 0.60 to 1.15. NACA RM L50C28, 1950.

TABLE I

SUMMARY OF INTEGRATED SECTION AND PANEL AERODYNAMIC CHARACTERISTICS

M	α, deg	Section normal-force coefficient c_n at station -						Section pitching-moment coefficient $c_{m_{c/4}}$ at station -						C_N	C_m	C_B	$\frac{x_{cp}}{c'}$	$\frac{y_{cp}}{b/2}$
		A	B	C	D	E	F	A	B	C	D	E	F					
M ≈ 0.70																		
0.688	-4.23	-0.181	-0.166	-0.163	-0.145	-0.089	-0.042	-0.032	-0.028	-0.026	-0.031	-0.027	-0.028	-0.136	-0.030	-0.050	-----	0.367
.698	-4.26	-.174	-.172	-.165	-.146	-.091	-.058	-.031	-.029	-.028	-.031	-.030	-.029	-.139	-.031	-.052	-----	.372
.688	-1.95	.050	.066	.079	.091	.104	.054	-.025	-.023	-.023	-.028	-.025	-.021	.077	-.025	.037	0.570	.478
.696	-1.96	.059	.073	.090	.102	.108	.060	-.025	-.025	-.024	-.028	-.028	-.020	.084	-.026	.040	.561	.479
.689	.33	.287	.314	.329	.339	.314	.183	-.018	-.018	-.020	-.025	-.022	-.013	.304	-.020	.130	.315	.488
.694	.33	.301	.320	.349	.353	.326	.185	-.017	-.020	-.020	-.025	-.023	-.014	.315	-.020	.136	.312	.431
.690	2.61	.527	.536	.581	.587	.533	.332	-.003	-.005	-.009	-.014	-.013	-.011	.531	-.007	.227	.264	.428
.695	2.60	.533	.573	.585	.590	.532	.325	-.003	-.006	-.009	-.013	-.013	-.013	.536	-.011	.227	.271	.422
.692	1.81	.737	.803	.830	.836	.751	.514	.016	.012	.007	.003	.004	-.011	.767	.009	.327	.259	.427
.696	4.90	.760	.815	.833	.838	.765	.504	.015	.011	.006	.003	.003	-.015	.769	.008	.327	.240	.425
.695	5.99	.857	.903	.941	.946	.866	.593	.021	.009	.005	0	.005	-.021	.871	.008	.375	.241	.430
.690	6.99	.663	.863	.888	.923	.897	.645	-.082	-.058	.005	0	.008	-.015	.843	-.027	.376	.284	.445
.697	6.93	.782	.899	.942	.970	.906	.640	-.013	-.010	.001	-.006	.007	-.023	.876	-.004	.385	.254	.439
.695	6.97	.728	.882	.891	.945	.899	.638	-.045	-.031	-.010	.003	.008	-.020	.851	-.016	.371	.268	.441
.694	7.96	.669	.905	.922	.970	.915	.680	-.083	-.068	.005	-.001	.008	-.024	.868	-.028	.388	.282	.447
.693	8.93	.618	.788	.893	.934	.914	.719	-.085	-.082	-.020	-.020	-.010	-.018	.829	-.048	.382	.307	.461
.697	8.91	.648	.879	.891	.926	.868	.651	-.086	-.070	-.019	-.094	-.018	-.021	.806	-.055	.357	.318	.443
.695	9.90	.617	.877	.850	.865	.872	.671	-.090	-.073	-.047	-.092	-.034	-.024	.818	-.063	.366	.327	.448
.689	10.87	.640	.707	.862	.851	.842	.699	-.083	-.097	-.062	-.088	-.102	-.035	.773	-.086	.359	.361	.464
.696	10.88	.625	.825	.862	.895	.851	.671	-.088	-.076	-.063	-.078	-.081	-.047	.806	-.074	.364	.341	.451
.692	12.91	.640	.668	.871	.813	.804	.708	-.085	-.103	-.083	-.118	-.133	-.056	.748	-.103	.346	.388	.463
.696	12.92	.676	.874	.906	.933	.798	.692	-.094	-.080	-.084	-.101	-.118	-.059	.832	-.089	.368	.357	.442
.690	13.94	0.663	0.693	0.914	0.877	0.795	0.728	-0.087	-0.105	-0.097	-0.118	-0.131	-0.064	0.778	-0.107	0.358	0.388	0.461
.691	14.96	.690	.722	.973	.955	.828	.775	-.091	-.109	-.105	-.115	-.130	-.081	.821	-.111	.380	.385	.463
.689	15.69	.709	.738	1.000	.970	.856	.801	-.093	-.111	-.110	-.118	-.131	-.096	.843	-.114	.390	.386	.463
M ≈ 0.73																		
.718	2.69	.553	.602	.614	.622	.571	.358	-.002	-.003	-.005	-.012	-.010	-.011	.567	-.005	.243	.259	.429
.721	2.66	.538	.587	.605	.609	.541	.341	.002	-.002	-.006	-.012	-.011	-.009	.555	-.005	.235	.259	.424
.718	4.98	.781	.829	.855	.863	.800	.548	.012	0	-.013	-.010	-.002	-.015	.794	-.003	.341	.254	.429
.721	4.92	.775	.833	.858	.861	.786	.535	.016	.007	-.001	-.007	-.003	-.014	.794	.003	.340	.247	.429
.721	6.07	.853	.908	.943	.949	.881	.622	.019	-.001	-.020	-.013	-.003	-.019	.879	-.005	.380	.256	.432
.718	7.02	.696	.865	.885	.919	.879	.658	-.053	-.043	-.014	-.035	-.002	-.018	.833	-.030	.371	.286	.445
.718	7.03	.724	.881	.925	.960	.914	.668	-.037	-.036	-.008	-.010	0	-.019	.870	-.020	.386	.273	.444
.718	7.97	.698	.853	.920	.972	.940	.713	-.065	-.073	-.005	-.013	-.002	-.021	.867	-.036	.392	.291	.452
.718	8.97	.629	.774	.873	.898	.903	.720	-.082	-.080	-.025	-.045	-.023	-.020	.814	-.053	.376	.315	.463
.718	10.94	.642	.762	.830	.812	.883	.731	-.083	-.080	-.068	-.119	-.065	-.028	.784	-.080	.362	.352	.462
.719	12.97	.662	.793	.889	.874	.835	.731	-.088	-.081	-.090	-.115	-.117	-.065	.808	-.095	.367	.368	.454
M ≈ 0.75																		
0.741	2.72	0.575	0.630	0.640	0.642	0.587	0.368	-0.002	-0.006	-0.009	-0.014	-0.010	-0.013	0.589	-0.008	0.252	0.263	0.427
.739	3.91	.702	.757	.775	.778	.715	.467	.004	-.004	-.016	-.017	-.007	-.016	.721	-.007	.308	.260	.428
.745	3.90	.712	.760	.774	.789	.729	.467	.003	-.005	-.030	-.018	-.010	-.019	.721	-.011	.308	.266	.428
.745	4.98	.762	.817	.834	.830	.781	.536	.007	-.020	-.041	-.029	-.006	-.018	.781	-.020	.336	.275	.430
.740	6.07	.823	.882	.881	.883	.845	.609	.008	-.034	-.052	-.048	-.010	-.020	.824	-.030	.360	.287	.437
.748	7.05	.813	.881	.882	.942	.913	.668	-.008	-.040	-.054	-.033	-.020	-.032	.859	-.035	.378	.290	.440
.744	8.95	.637	.834	.847	.801	.861	.686	-.081	-.068	-.039	-.097	-.030	-.019	.800	-.060	.356	.325	.445
M ≈ 0.80																		
0.800	-4.39	-0.233	-0.234	-0.229	-0.215	-0.168	-0.097	-0.039	-0.035	-0.032	-0.034	-0.039	-0.035	-0.202	-0.035	-0.080	-----	0.396
.794	-1.95	.068	.096	.101	.109	.111	.055	-.031	-.032	-.032	-.038	-.033	-.024	.094	-.033	.042	.606	.451
.799	-1.95	.073	.086	.098	.111	.107	.062	-.034	-.034	-.036	-.040	-.041	-.026	.092	-.036	.042	.639	.457
.793	.45	.352	.386	.408	.411	.369	.217	-.029	-.034	-.041	-.047	-.038	-.022	.369	-.037	.157	.350	.426
.793	2.77	.583	.631	.646	.644	.592	.381	-.017	-.042	-.063	-.068	-.040	-.026	.594	-.046	.253	.388	.426
.800	3.92	.688	.736	.715	.707	.681	.458	-.025	-.059	-.057	-.076	-.048	-.033	.676	-.052	.288	.327	.425
.799	3.92	.691	.739	.724	.715	.692	.463	-.025	-.059	-.057	-.076	-.048	-.034	.686	-.052	.293	.326	.427
.797	5.01	.752	.798	.765	.786	.772	.539	-.035	-.055	-.062	-.083	-.049	-.039	.752	-.056	.316	.324	.421
.798	6.08	.796	.843	.841	.835	.830	.603	-.036	-.059	-.076	-.079	-.052	-.043	.804	-.059	.349	.324	.434
.798	7.13	.829	.857	.874	.870	.887	.664	-.038	-.068	-.068	-.087	-.066	-.055	.841	-.065	.369	.328	.439
.799	7.15	.830	.869	.849	.905	.912	.677	-.035	-.060	-.077	-.067	-.076	-.056	.846	-.064	.372	.326	.440
.798	8.05	.637	.831	.871	.891	.906	.692	-.078	-.078	-.042	-.078	-.063	-.049	.822	-.066	.373	.331	.453
.798	9.06	.626	.870	.892	.906	.942	.739	-.084	-.078	-.049	-.080	-.071	-.052	.852	-.070	.388	.332	.456
M ≈ 0.85																		
0.845	-4.41	-0.242	-0.234	-0.233	-0.215	-0.156	-0.100	-0.027	-0.019	-0.012	-0.017	-0.028	-0.035	-0.202	-0.022	-0.079	-----	0.391
.848	-4.40	-.235	-.235	-.222	-.192	-.156	-.093	-.029	-.022	-.018	-.016	-.034	-.035	-.195	-.025	-.075	-----	.386
.842	-1.99	.044	.066	.073	.076	.093	.050	-.042	-.047	-.051	-.054	-.051	-.032	.070	-.048	.033	.929	.472
.850	-2.02	.066	.073	.073	.089	.100	.057	-.047	-.048	-.051	-.054	-.052	-.032	.078	-.049	.036	.880	.463
.842	.41	.309	.339	.345	.340	.337	.205	-.049	-.065	-.073	-.074	-.072	-.034	.323	-.064	.139	.448	.429
.847	2.71	.534	.562	.532	.503	.531	.355	-.057	-.066	-.067	-.070	-.081	-.044	.513	-.065	.218	.376	.425
.845	4.92	.671	.700	.709	.690	.727	.518	-.049	-.076	-.076	-.083	-.095	-.061	.679	-.075	.298	.361	.439
.844	4.94	.664	.721	.701	.708	.733	.517	-.053	-.070	-.079	-.085	-.099	-.071	.682	-.077	.297	.363	.436
.844	7.12	.775	.848	.836	.840	.880	.673	-.055	-.076	-.086	-.092	-.112	-.091	.822	-.085	.365	.353	.444
.848	7.13	.778	.840	.776	.851	.858	.664	-.057	-.070	-.088	-.090	-.106	-.091	.800	-.083	.351	.354	.439
.847	8.17	.782	.842	.875	.871	.921	.730	-.056	-.079	-.085	-.092	-.118	-.095	.851	-.086	.383	.351	.450
.845	8.20	.850	.890	.840	.909	.926	.736	-.062	-.081	-.094	-.095	-.116	-.102	.863	-.092	.382	.356	.443
.847	9.08	.642	.752	.888	.895	.936	.756	-.078	-.086	-.074	-.090	-.106	-.085	.825	-.087	.386	.355	.468
.847	9.13	.656	.835	.913	.923	.950	.768	-.085	-.088	-.077	-.096	-.110	-.096	.850	-.093	.389	.359	.457

NACA

TABLE I - Concluded

SUMMARY OF INTEGRATED SECTION AND PANEL AERODYNAMIC CHARACTERISTICS - Concluded

M	α, deg	Section normal-force coefficient c_n at station -						Section pitching-moment coefficient $c_{m_{c/4}}$ at station -						C_N	C_m	C_B	$\frac{x_{cp}}{c'}$	$\frac{y_{cp}}{b/2}$
		A	B	C	D	E	F	A	B	C	D	E	F					
M ≈ 0.90																		
0.897	-4.38	-0.217	-0.242	-0.121	-0.185	-0.224	-0.109	-0.035	-0.010	-0.062	-0.019	-0.002	-0.028	-0.185	-0.027	0.031	0.104	0.081
.896	-2.13	-.091	-.121	-.038	-.083	-.109	-.007	.006	.032	-.011	.029	-.026	-.012	-.087	.004	.016	.296	.069
.896	-2.10	-.011	-.062	-.082	-.022	.010	.020	-.020	.011	.029	-.002	-.010	-.019	-.033	.003	-.008	.325	-----
.897	.17	.093	.113	.110	.086	.092	.117	.014	.023	.024	.034	.018	-.008	.102	.021	.019	.044	.441
.899	2.57	.320	.354	.350	.338	.304	.235	.001	.002	-.005	-.004	-.006	-.018	.323	-.002	.056	.256	.424
.898	4.84	.538	.588	.570	.548	.570	.422	-.018	-.034	-.040	-.035	-.054	-.052	.547	-.036	.100	.316	.433
.897	7.21	.837	.834	.825	.815	.806	.609	-.082	-.100	-.109	-.113	-.109	-.090	.791	-.100	.142	.376	.430
.895	8.34	.942	1.000	.957	.979	.966	.697	-.104	-.150	-.148	-.161	-.167	-.128	.940	-.146	.405	.405	.431
M ≈ 0.95																		
.939	-4.45	-0.266	-0.246	-0.245	-0.242	-0.197	-0.087	0.003	0.004	0.012	0.014	0.001	-0.029	-0.219	0.003	-0.087	-----	-----
.950	-2.12	-.024	-.011	-.014	-.020	.002	.017	-.022	-.020	-.015	-.011	-.019	-.027	-.009	-.018	-.002	-----	0.187
.942	.28	.230	.243	.236	.223	.216	.141	-.052	-.051	-.049	-.045	-.046	-.027	.216	-.047	.091	0.467	.422
.941	2.66	.466	.489	.481	.450	.422	.262	-.077	-.083	-.088	-.079	-.073	-.031	.436	-.076	.181	.424	.414
.940	4.97	.703	.738	.719	.683	.644	.406	-.111	-.131	-.134	-.122	-.112	-.046	.672	-.117	.281	.423	.419
.942	7.21	.896	.958	.925	.896	.842	.552	-.138	-.183	-.179	-.173	-.153	-.070	.863	-.160	.362	.435	.420
M ≈ 1.00																		
0.995	-4.44	-0.265	-0.261	-0.257	-0.246	-0.204	-0.103	-0.001	0.013	0.023	0.020	0.003	-0.022	-0.230	0.009	0.035	0.290	0.100
.990	-2.04	-.012	.006	.001	-.008	.028	.022	-.024	-.025	-.019	-.014	-.026	-.027	.006	-.023	.005	-----	-----
.991	.33	.218	.234	.225	.208	.206	.128	-.049	-.050	-.046	-.042	-.042	-.023	.207	-.044	.087	.463	-----
.995	2.72	.458	.482	.477	.463	.423	.270	-.084	-.083	-.091	-.088	-.081	-.034	.465	-.080	.092	.422	.447
.993	5.01	.681	.710	.689	.653	.619	.392	-.107	-.122	-.123	-.111	-.100	-.046	.636	-.107	.266	.418	.418
.998	5.04	.688	.701	.679	.666	.626	.386	-.108	-.116	-.117	-.120	-.105	-.041	.638	-.106	.265	.417	.416

NACA

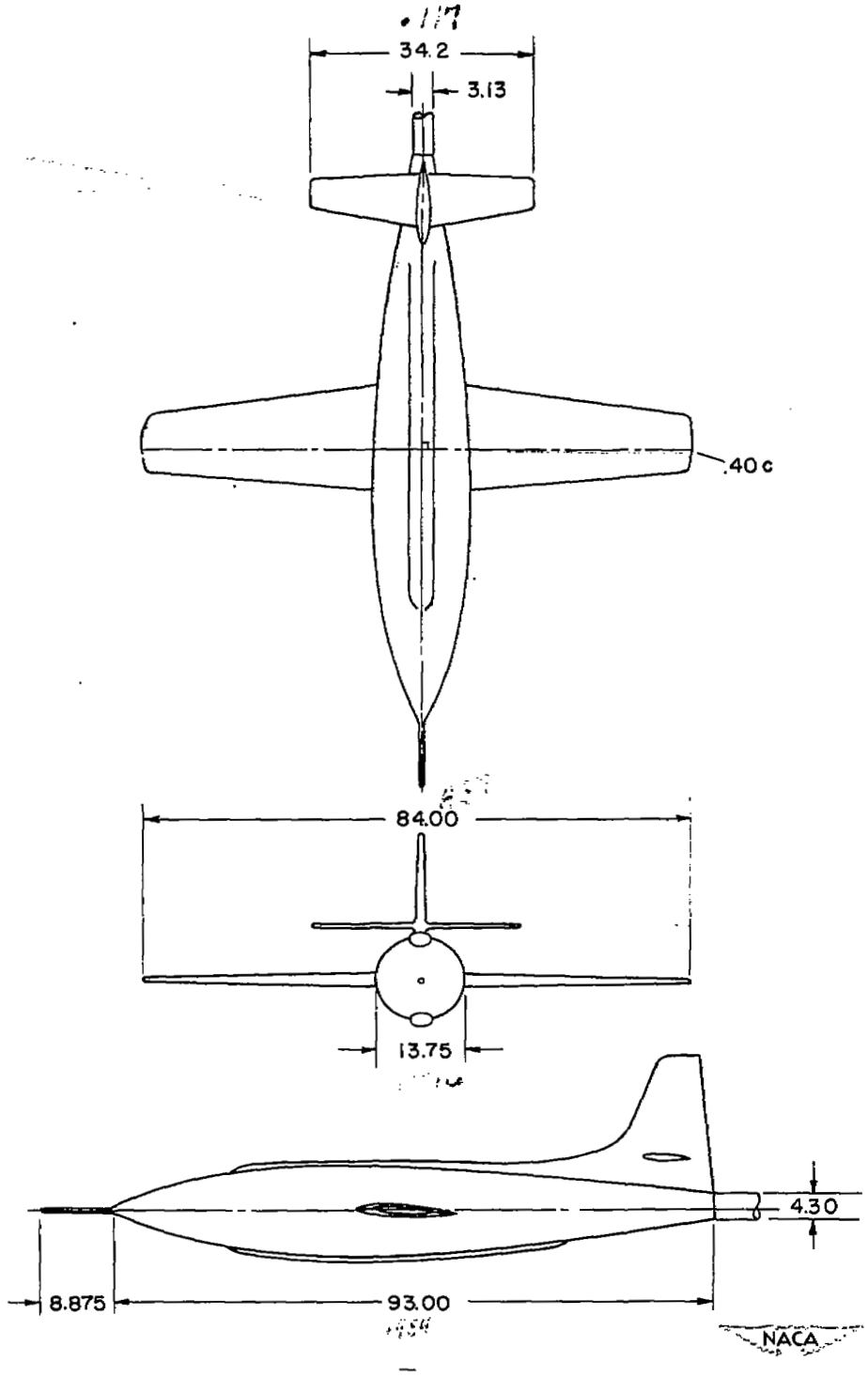

(a) Model dimensions.

Figure 1.- Sketch of $\frac{1}{4}$-scale model of the X-1-2 airplane as tested in the Langley 16-foot transonic tunnel. All dimensions in inches.

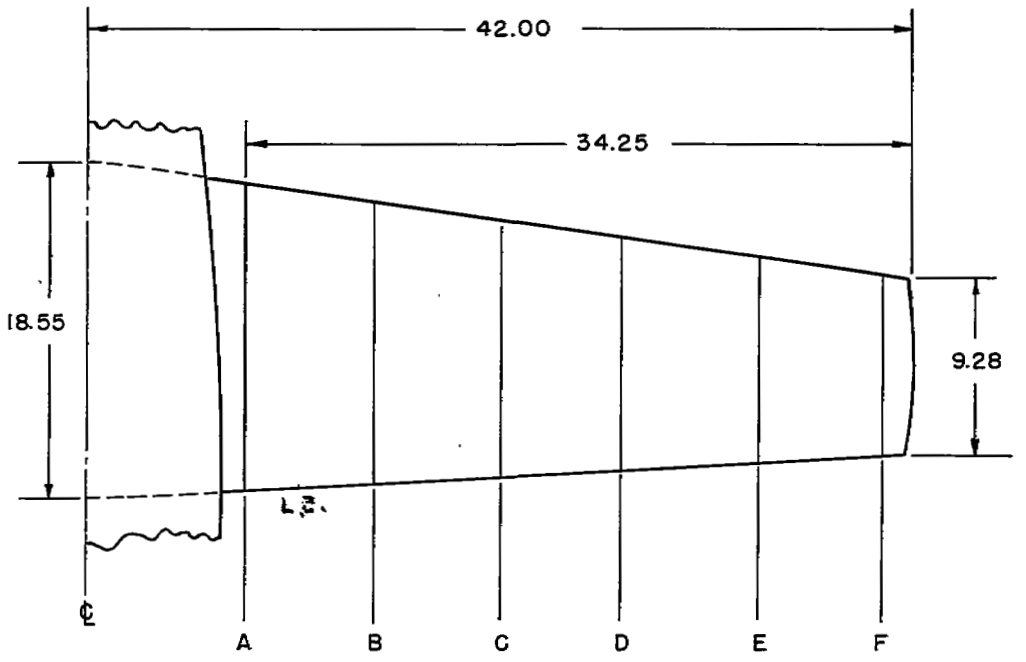

Spanwise locations of pressure measuring orifices

Span. station	A	B	C	D	E	F
Distance from model center line, percent semispan	18.5	33.8	49.1	64.4	79.8	95.1
Distance from station A, percent semispan	0	18.8	37.6	56.4	75.2	94.0

Chordwise locations of pressure measuring orifices (percent chord)

The distribution of orifices at all spanwise stations is identical.

Upper surface 0, 1.25, 2.5, 5, 7.5, 10, 15, 20, 25, 30, 35, 40, 45, 50, 55, 60, 65, 70, 75, 80, 85, 90, 95
Lower surface 1.25, 2.5, 5, 7.5, 10, 15, 20, 25, 30, 35, 40, 45, 50, 55, 60, 65, 70, 75, 80, 85, 90, 95

Local wing station incidence

Span station	℄	A	B	C	D	E	F
Incidence, degrees	2.50	2.40	2.30	2.17	2.02	1.86	1.51

(b) Wing dimensions.

Figure 1.- Continued.

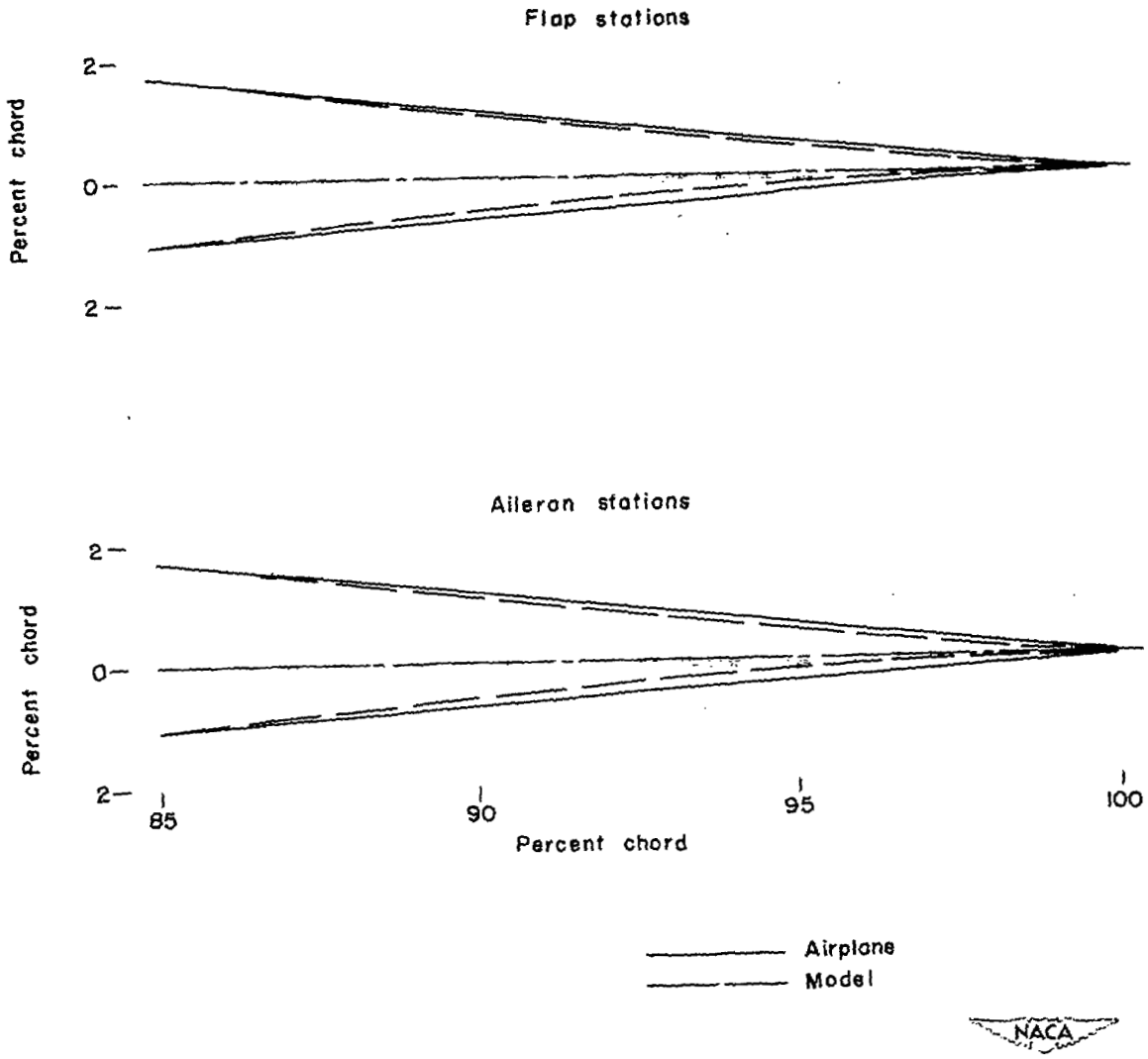

(c) Physical differences between airplane and model wing trailing edge.

Figure 1.- Concluded.

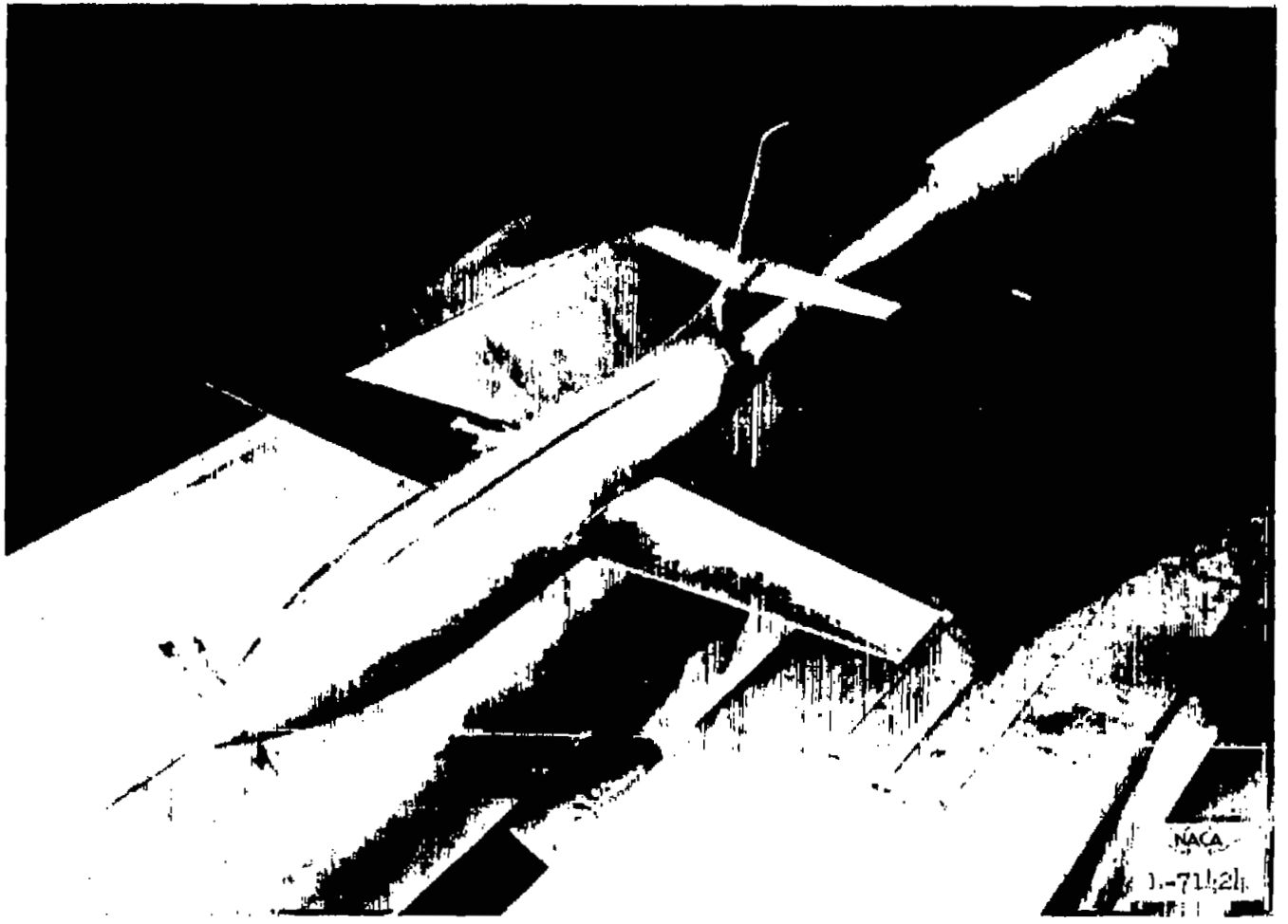

(a) Three-quarter front view.

Figure 2.- The $\frac{1}{4}$-scale model of the X-1-2 airplane and the model support system in the Langley 16-foot transonic tunnel.

(b) Three-quarter rear view.

Figure 2.- Concluded.

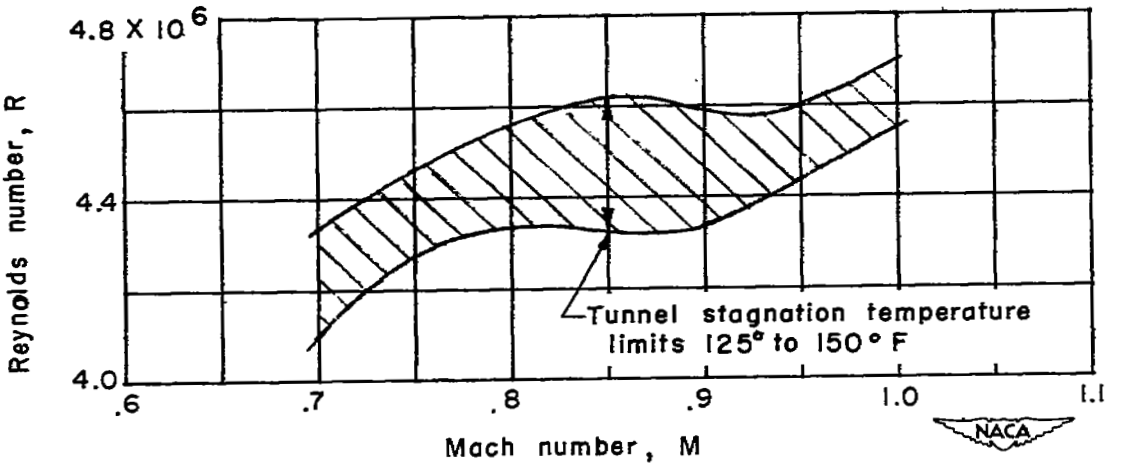

Figure 3.- Variation of Reynolds number with Mach number obtained in the investigation of a $\frac{1}{4}$-scale model of the X-1-2 airplane in the Langley 16-foot transonic tunnel. c' = 1.203 feet.

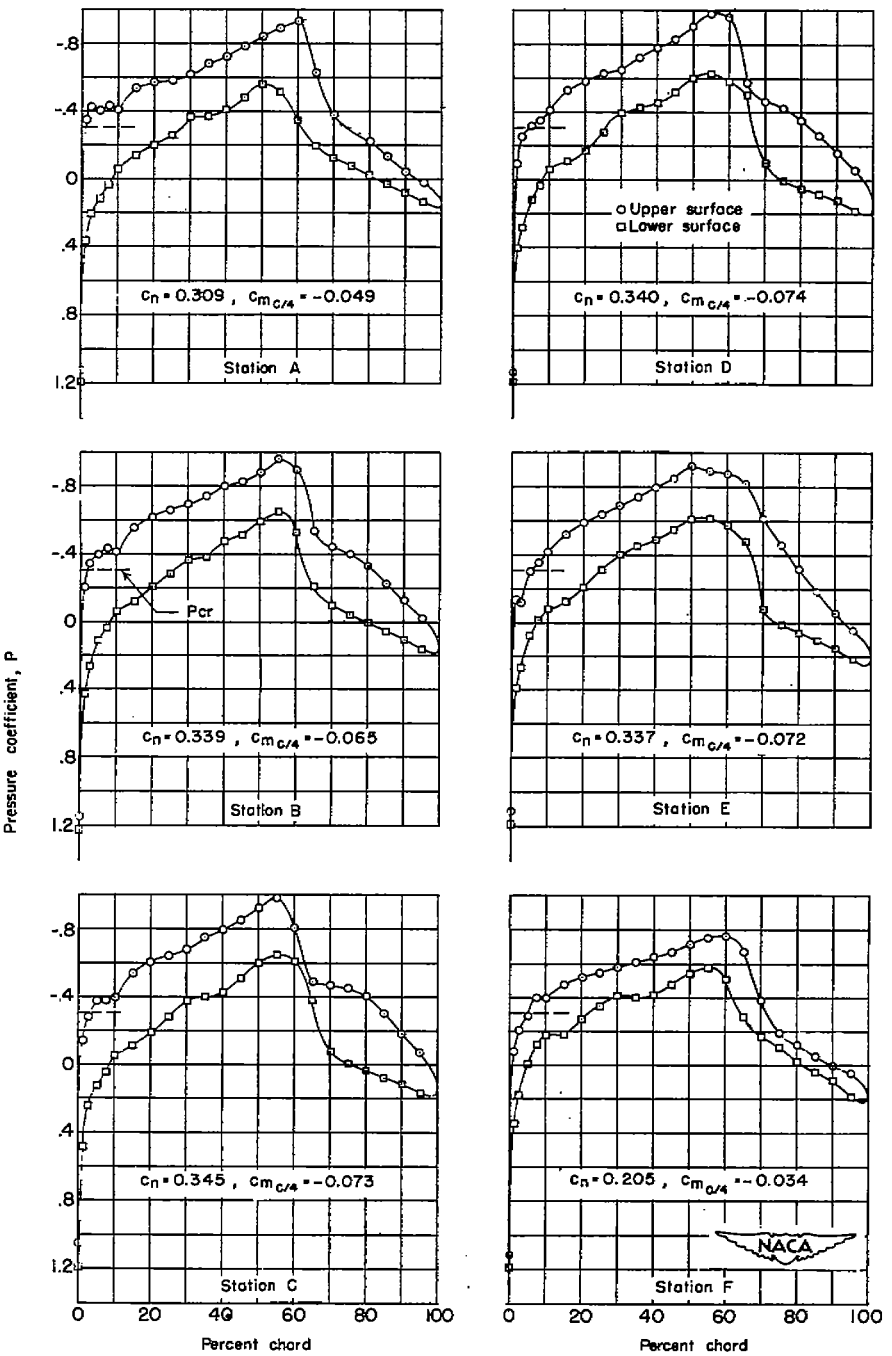

(a) $\alpha = 0.4^\circ$; $C_N = 0.323$.

Figure 4.- Chordwise pressure distributions over the left wing of the $\frac{1}{4}$-scale model of the X-1-2 airplane at $M \approx 0.85$.

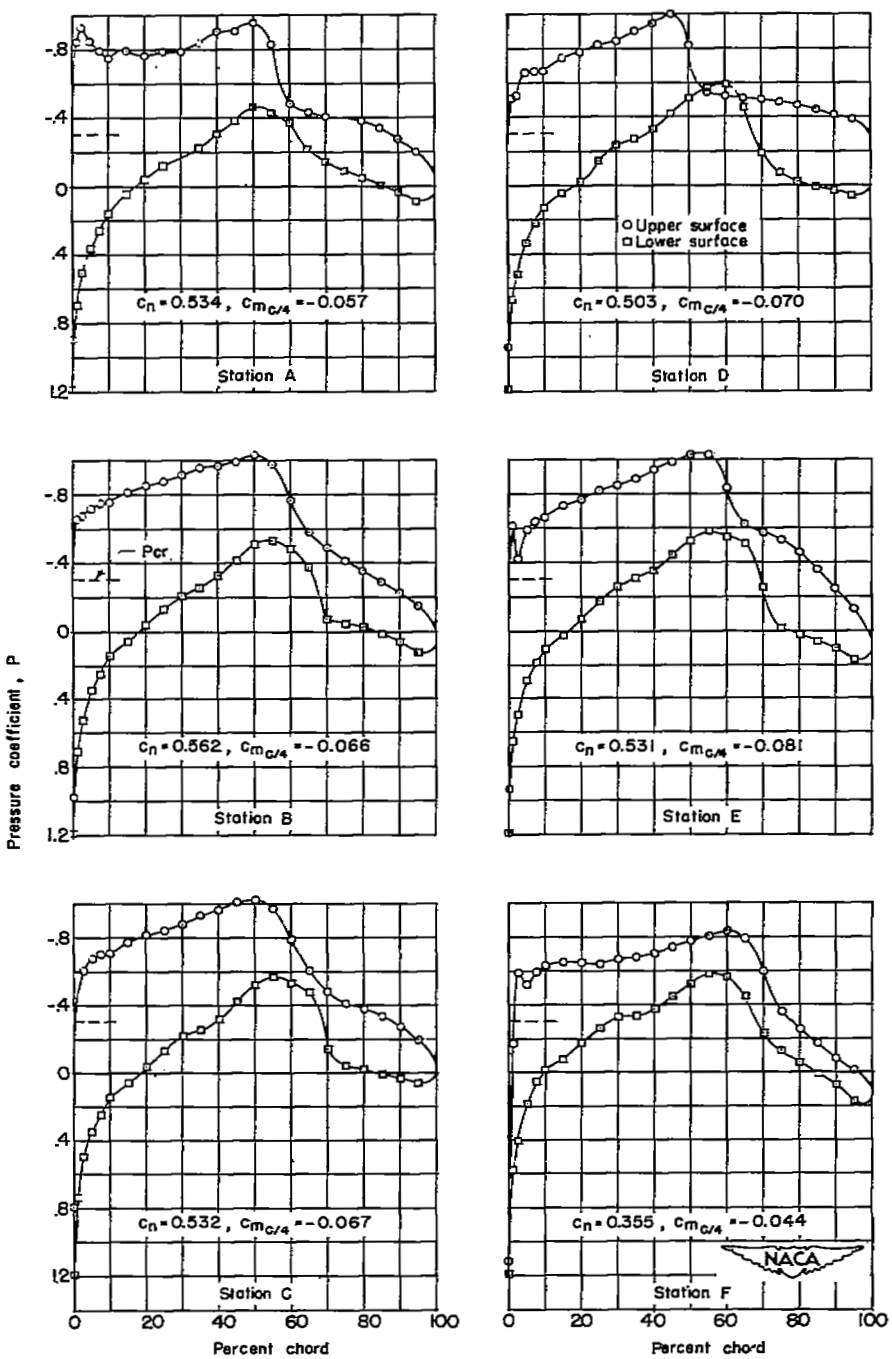

(b) $\alpha = 2.7^{\circ}$; $C_N = 0.513$.

Figure 4.- Continued.

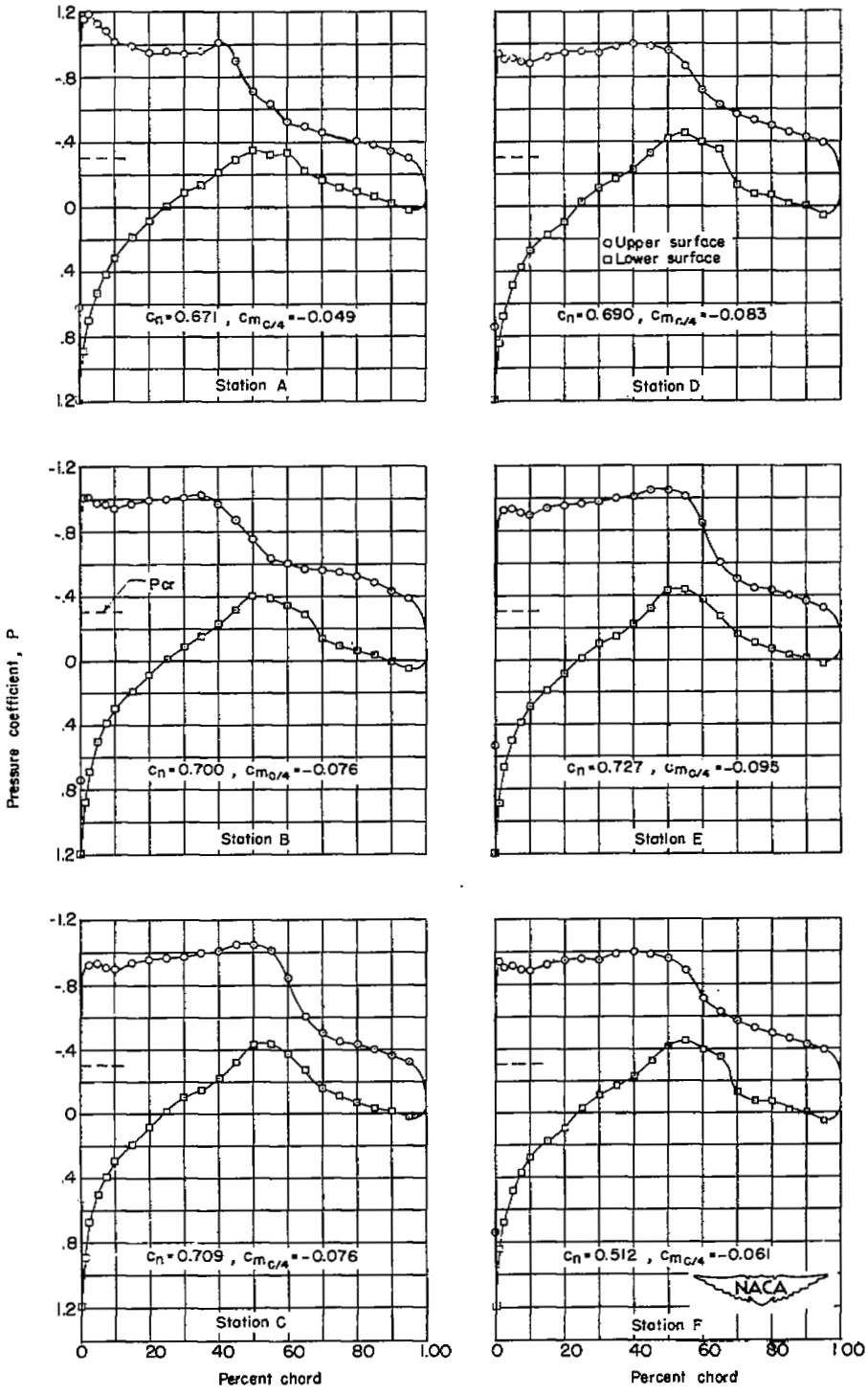

(c) $\alpha = 4.9^{\circ}$; $C_N = 0.679$.

Figure 4.- Concluded.

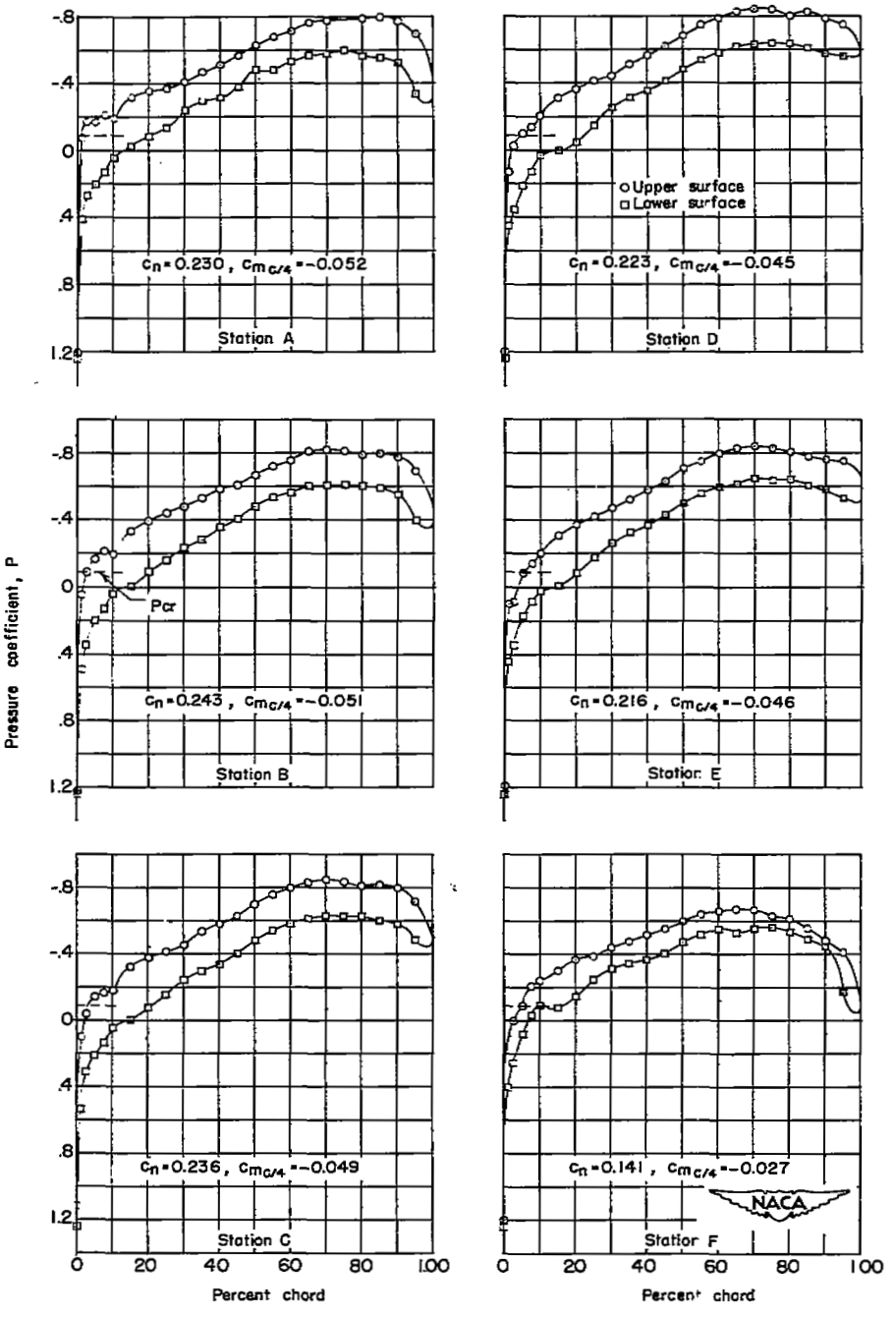

(a) $\alpha = 0.3^{\circ}$; $C_N = 0.216$.

Figure 5.- Chordwise pressure distributions over the left wing of the $\frac{1}{4}$-scale model of the X-1-2 airplane at $M \approx 0.95$.

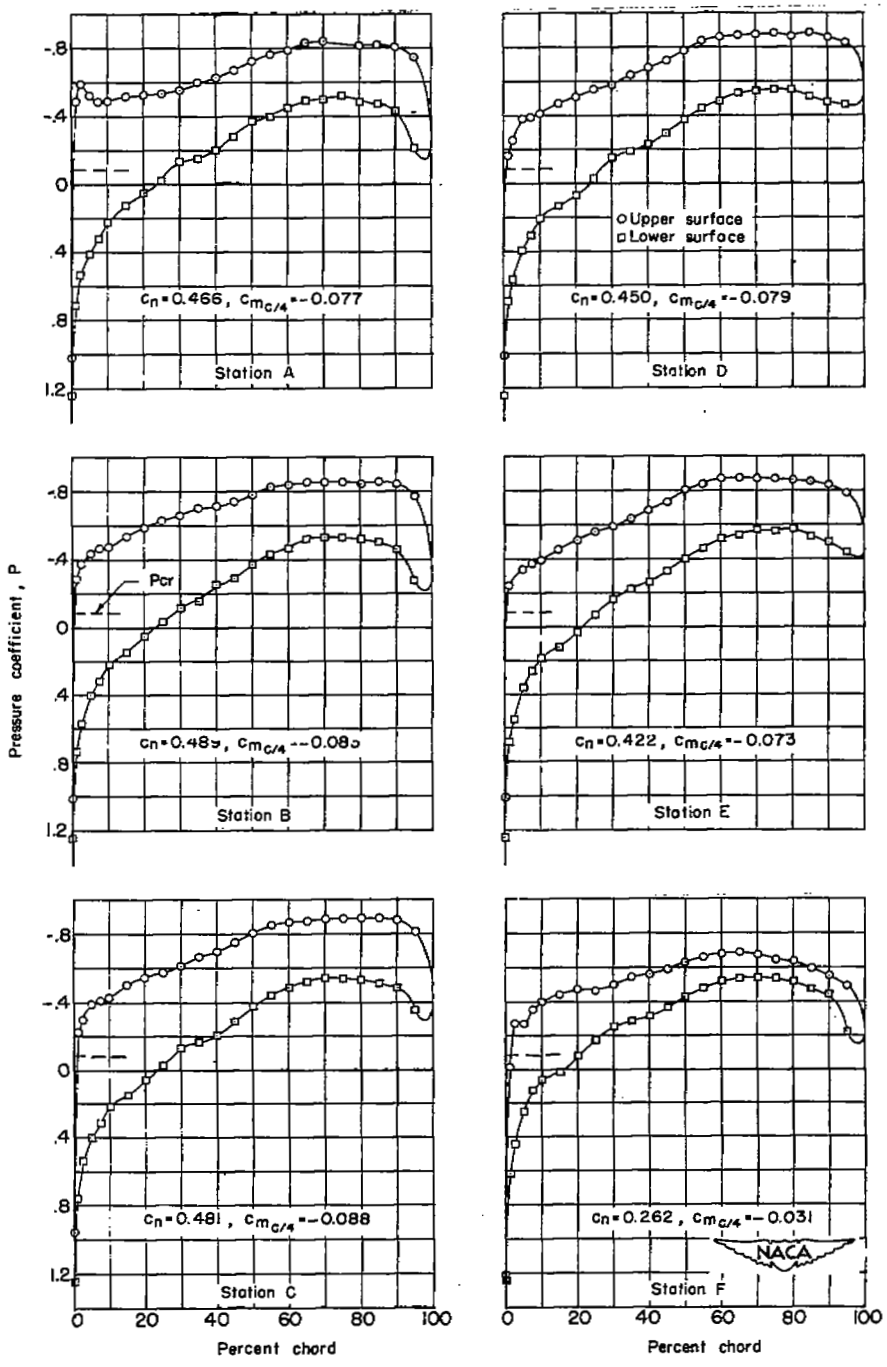

(b) $\alpha = 2.7^{\circ}$; $C_N = 0.436$.

Figure 5.- Continued.

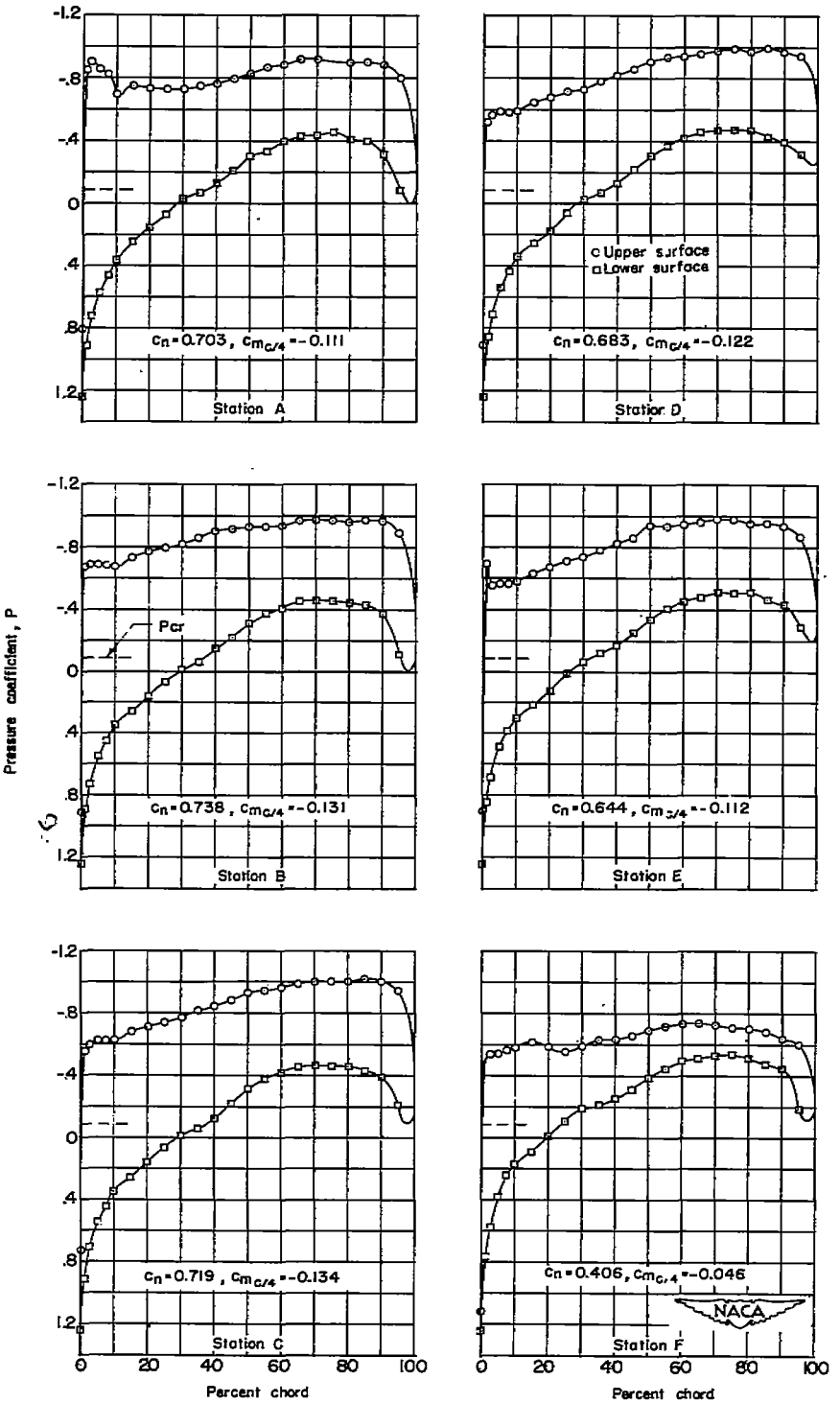

(c) $\alpha = 5.0^{\circ}$; $C_N = 0.672$.

Figure 5.- Concluded.

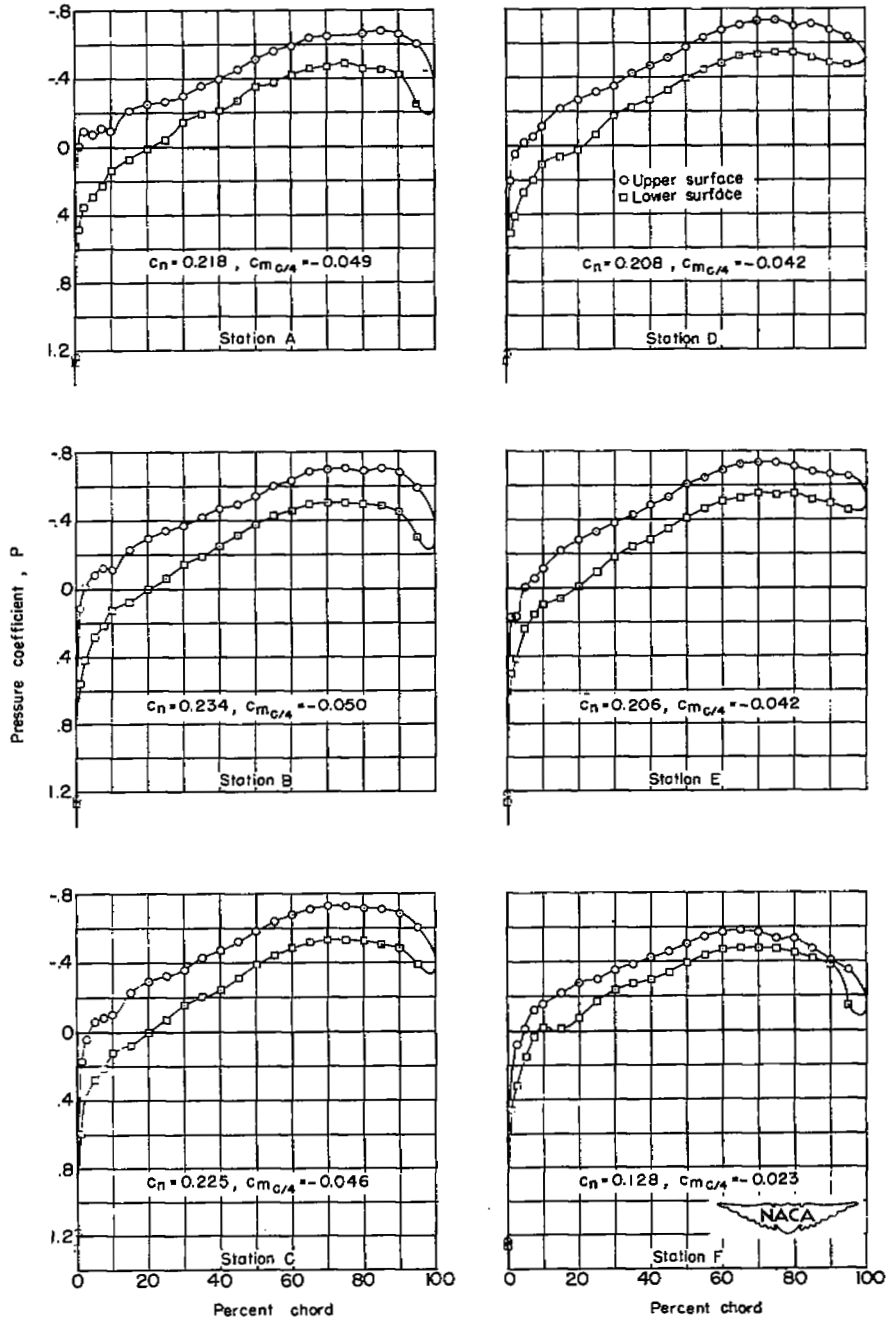

(a) $\alpha = 0.3^{\circ}$; $C_N = 0.207$.

Figure 6.- Chordwise pressure distributions at transonic speeds over the left wing of the $\frac{1}{4}$-scale model of the X-1-2 airplane at $M \approx 1.00$.

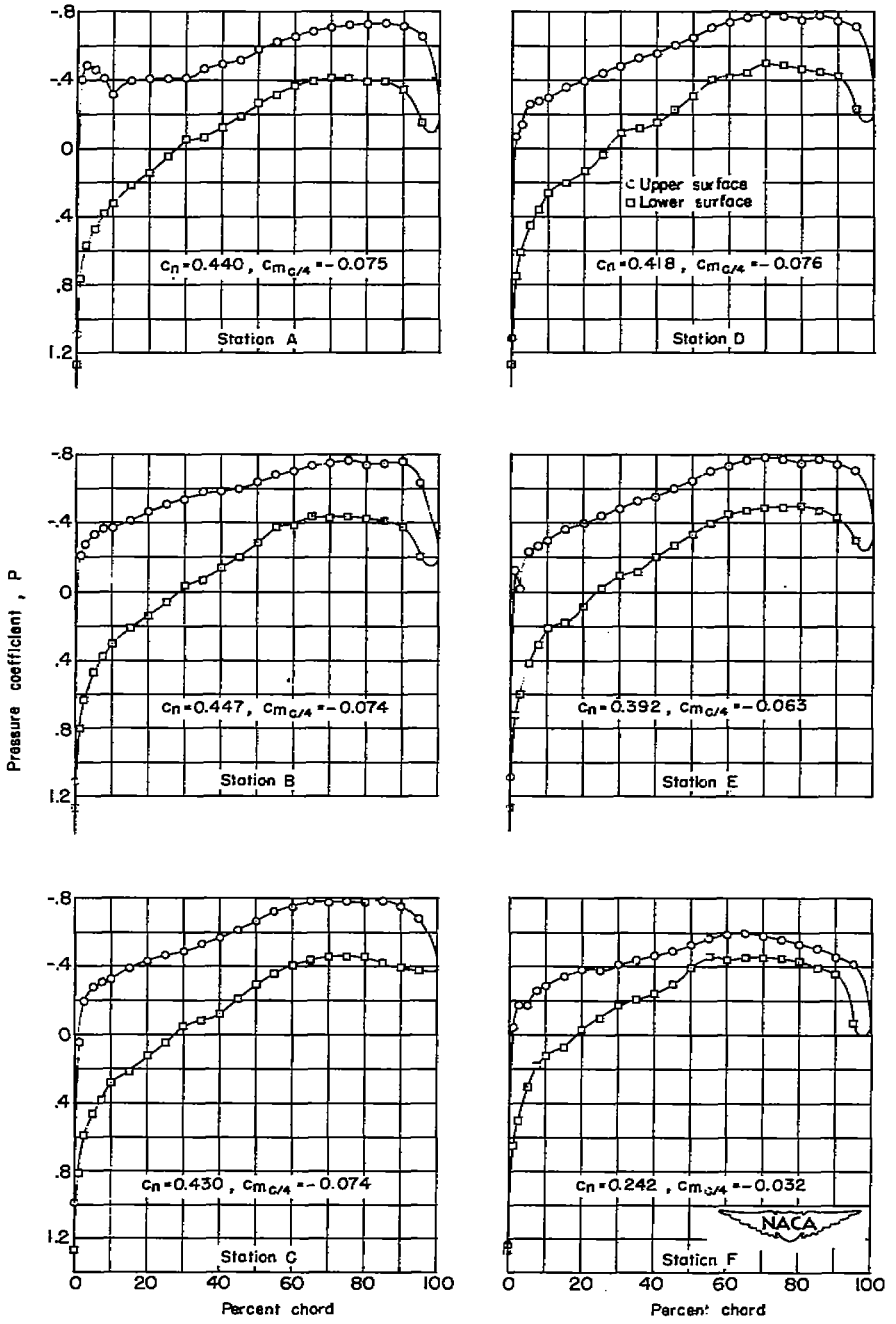

(b) $\alpha = 2.6^{\circ}$; $C_L = 0.417$; $C_N = 0.407$.

Figure 6.- Continued.

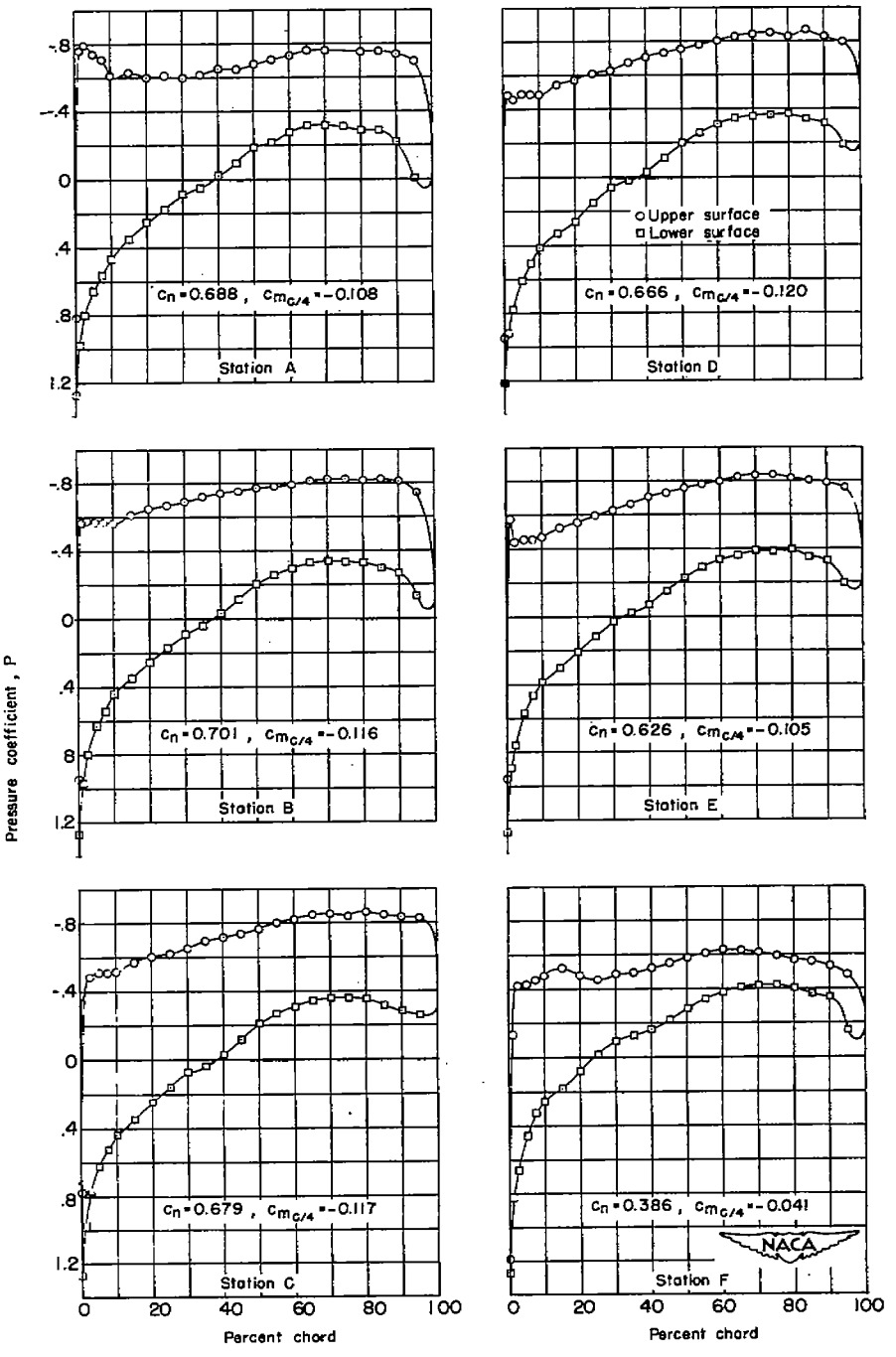

(c) $\alpha = 5.0^{\circ}$; $C_N = 0.638$.

Figure 6.- Concluded.

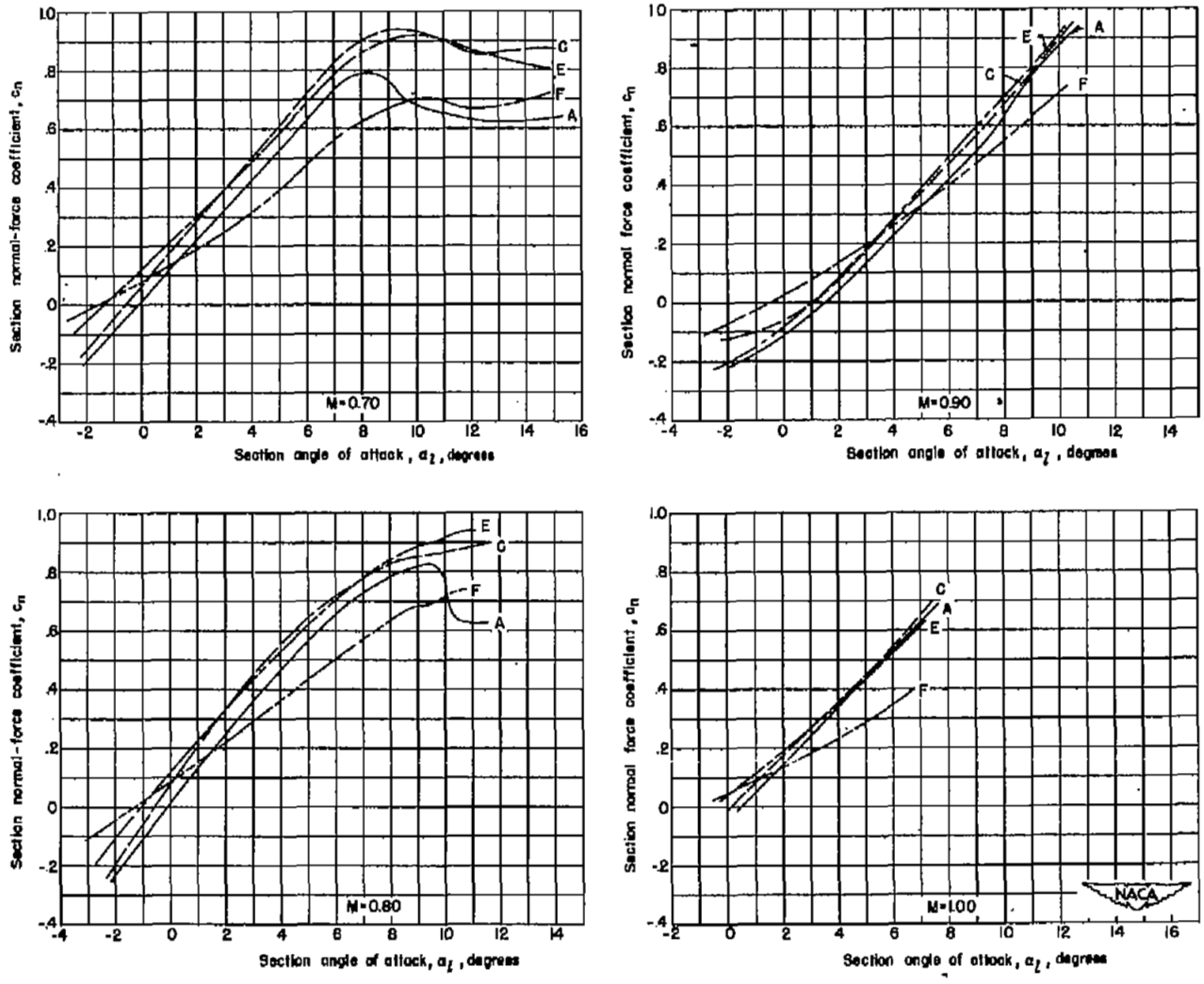

Figure 7.- Section normal-force curves for stations A, C, E, and F at several Mach numbers.

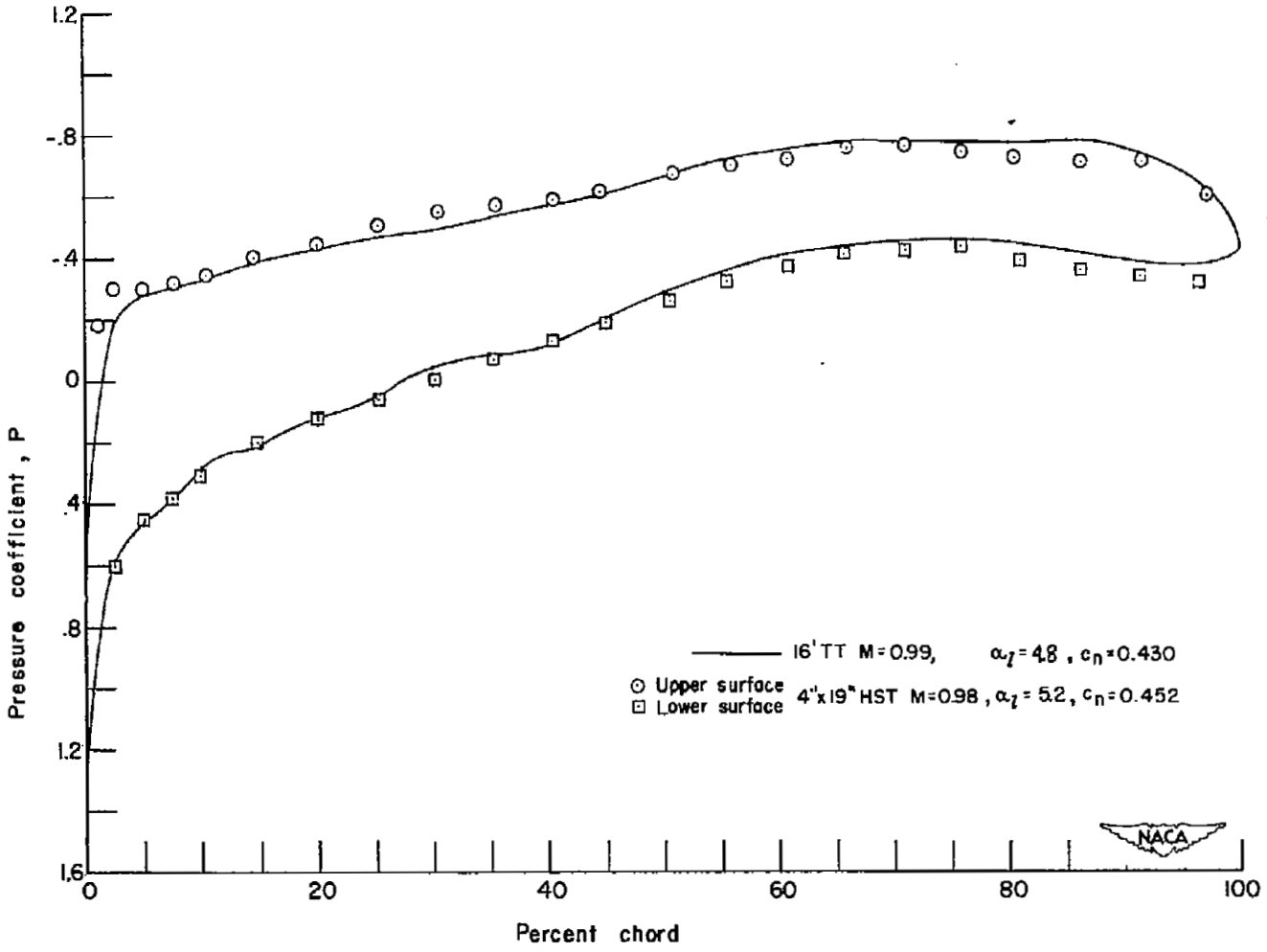

Figure 8.- Comparison of pressure distribution obtained at station C with two-dimensional data near M = 1.0. Langley 16-foot transonic tunnel data angle of attack corrected for air-stream angularity.

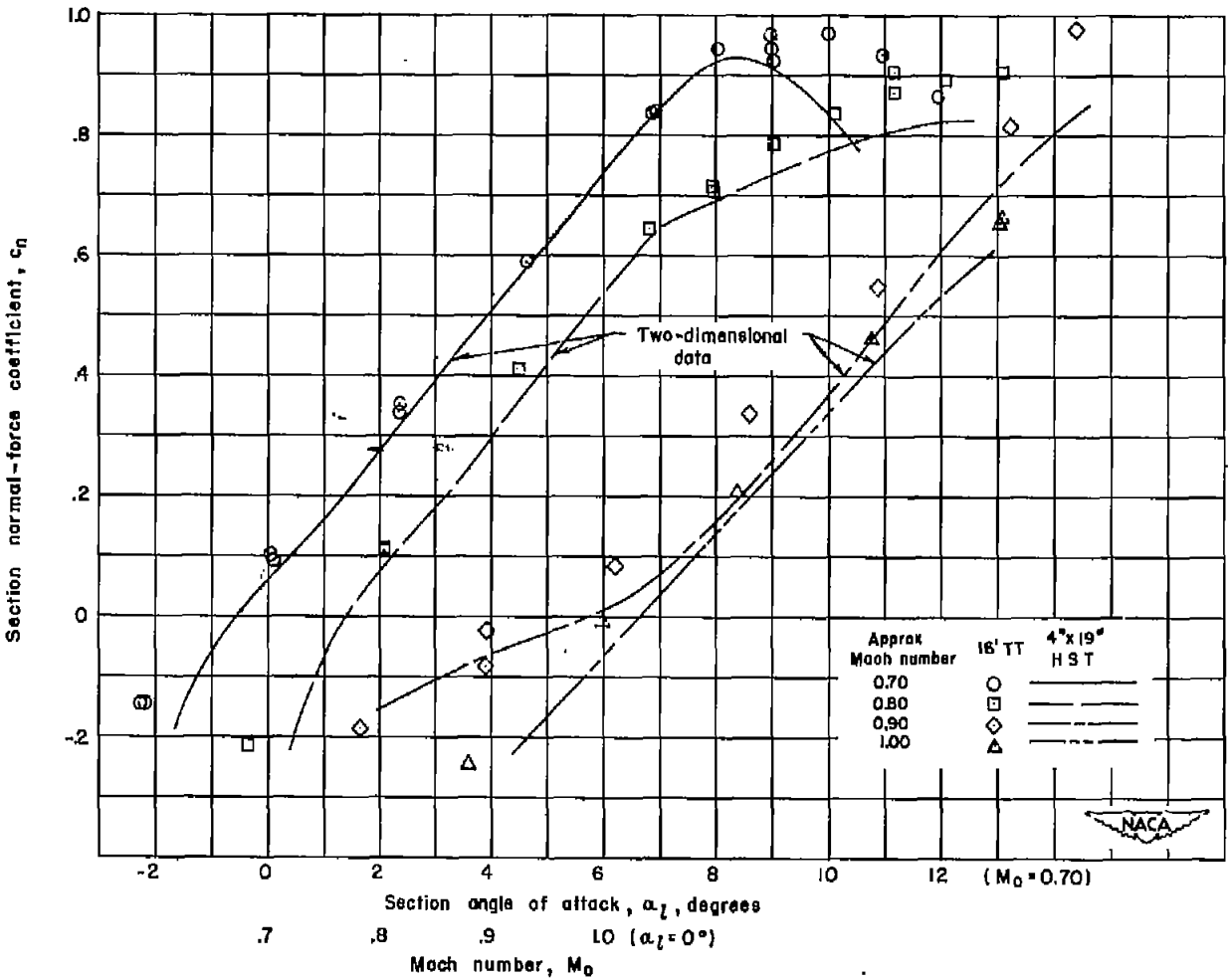

Figure 9.- Comparison at several Mach numbers of the section normal-force curves for station D with data obtained in the Langley 4- by 19-inch high-speed tunnel. Langley 16-foot transonic tunnel angle of attack corrected for stream angularity.

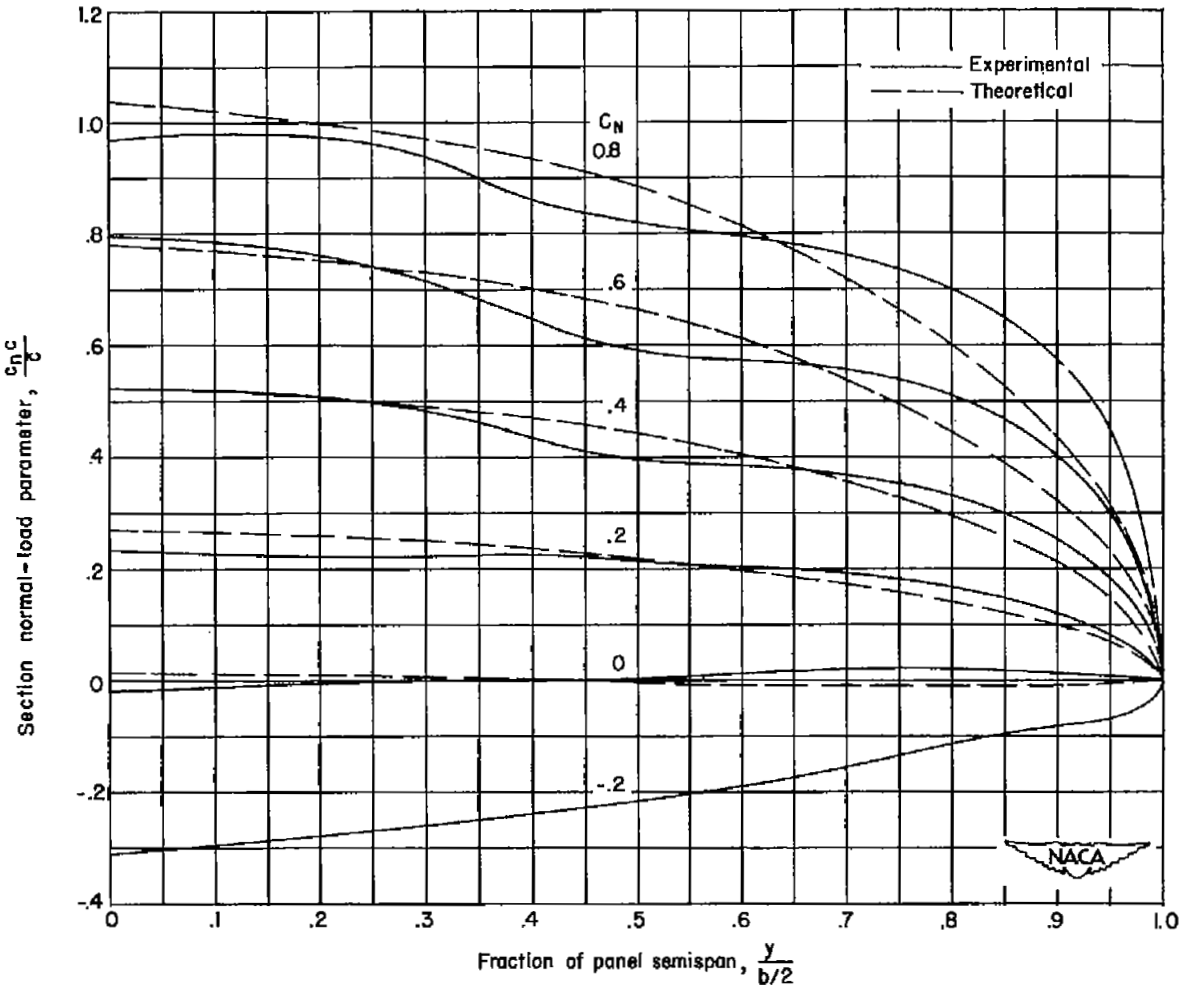

(a) M ≈ 0.85.

Figure 10.- Variation of span-load distributions with normal-force coefficient for several Mach numbers.

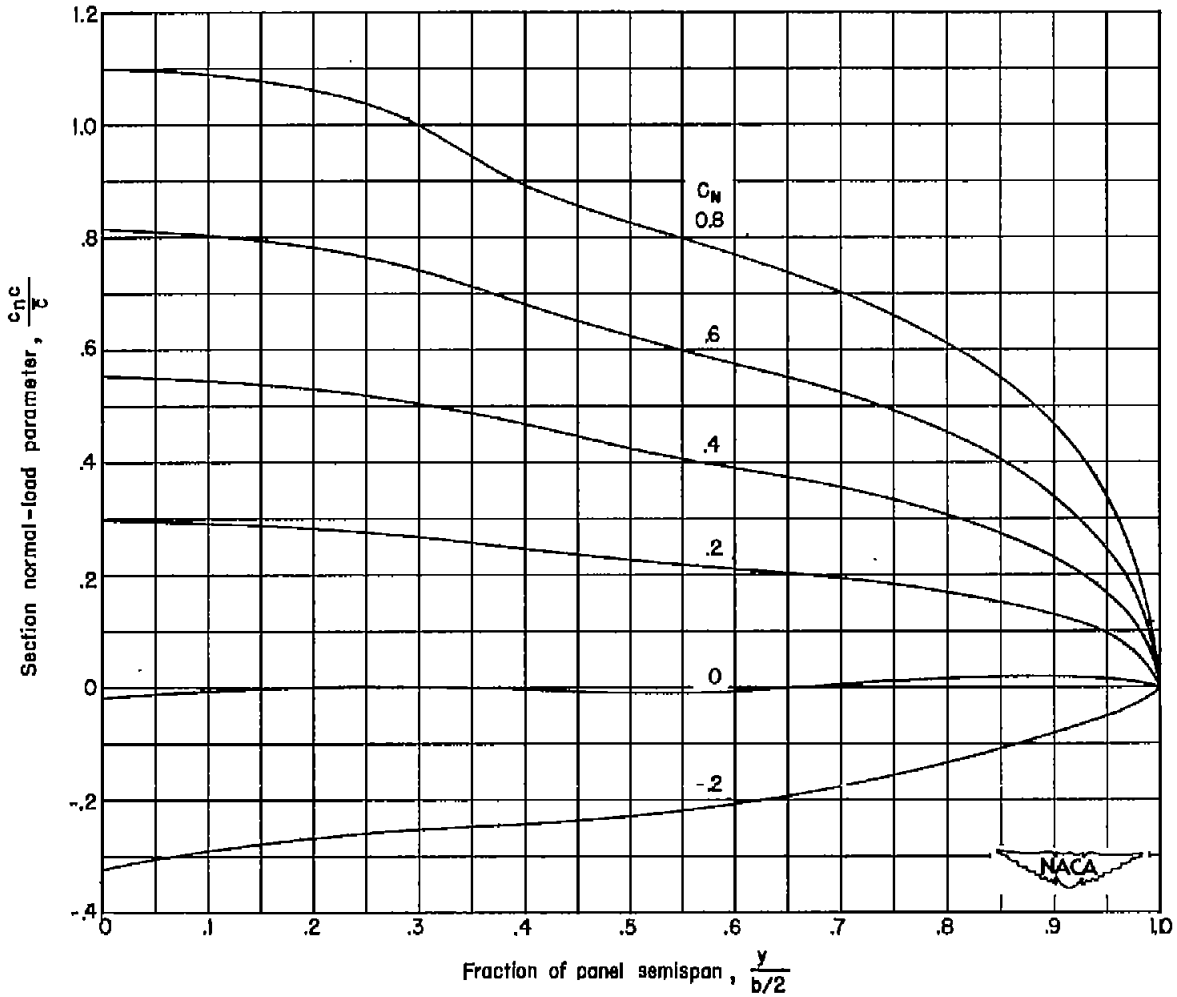

(b) M ≈ 0.95.

Figure 10.- Continued.

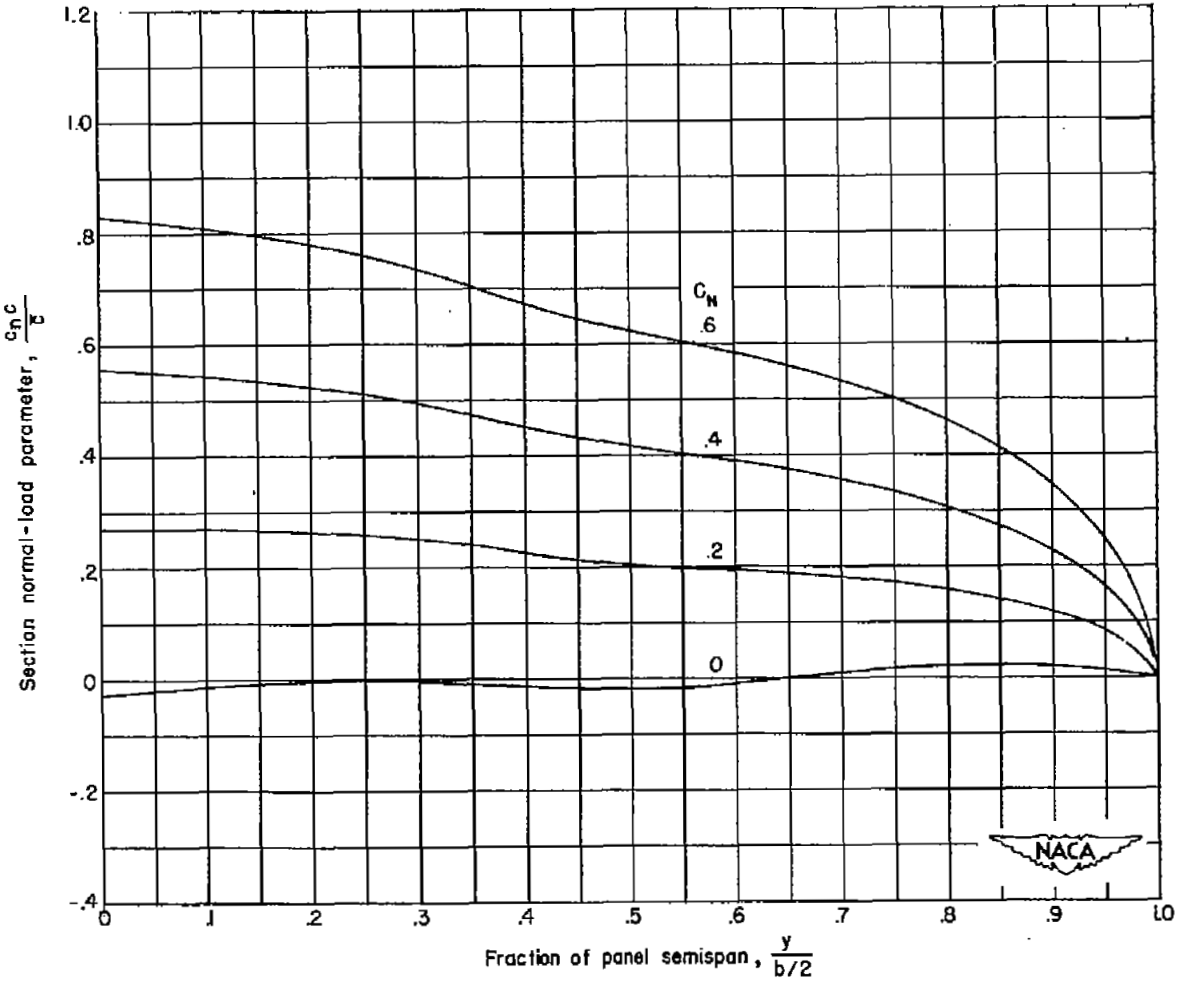

(c) M ~ 1.00.

Figure 10.- Concluded.

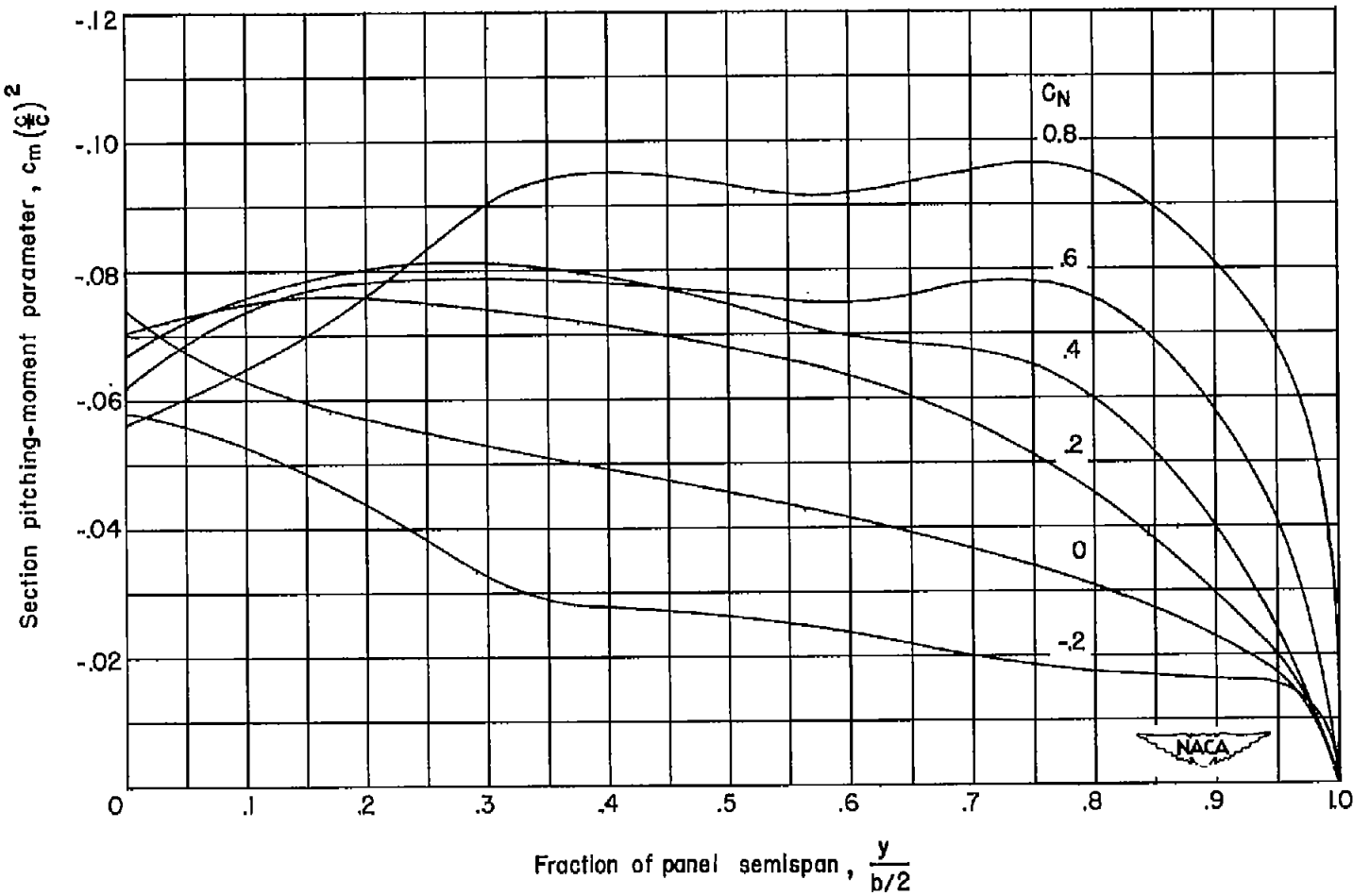

(a) $M \approx 0.85$.

Figure 11.- Spanwise variation of section pitching-moment parameters with normal-force coefficient for several Mach numbers.

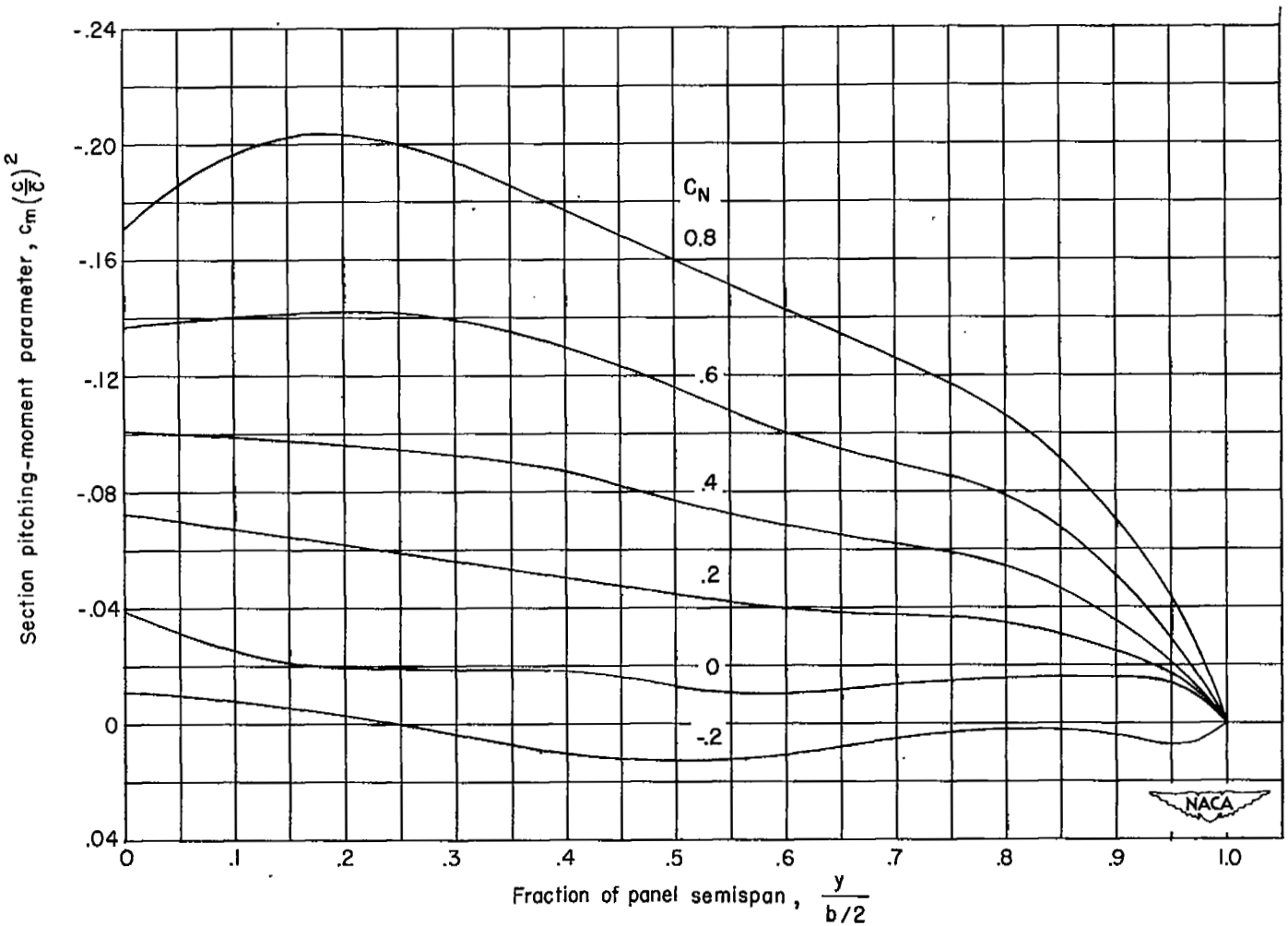

(b) $M \approx 0.95$.

Figure 11.- Continued.

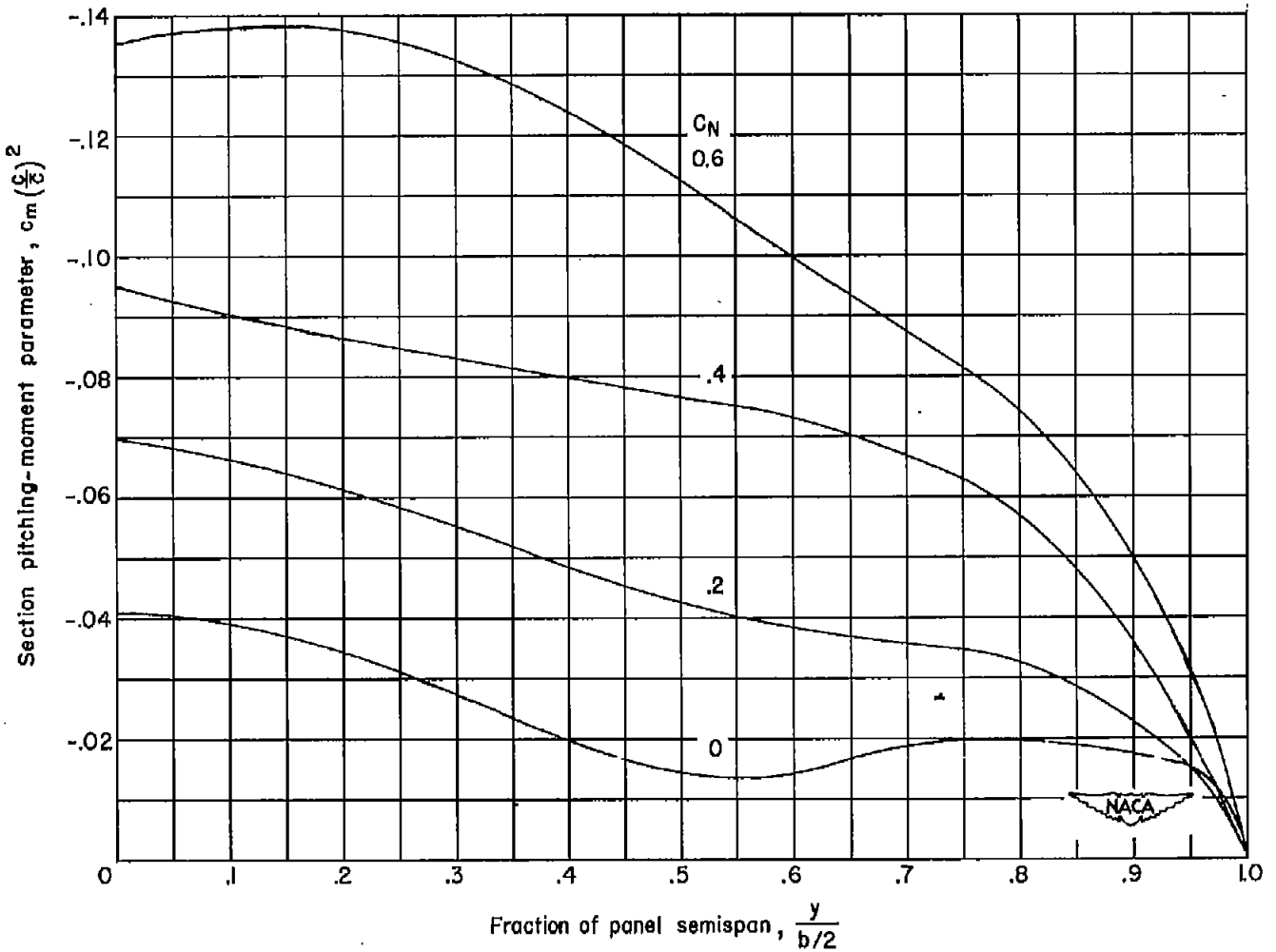

(c) M ≈ 1.00.

Figure 11.- Concluded.

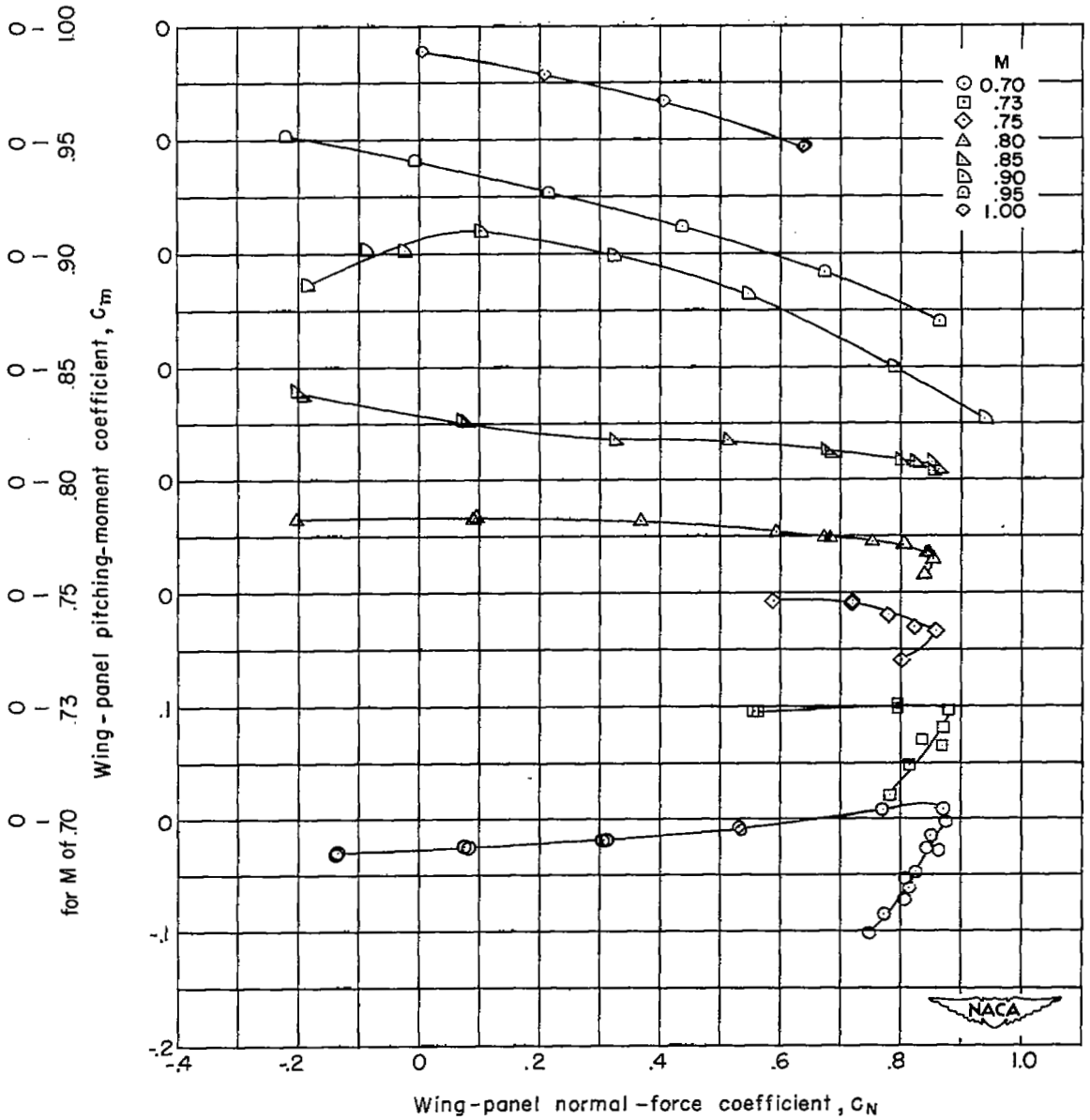

Figure 12.- Variation of wing-panel pitching-moment coefficient with wing-panel normal-force coefficient for several Mach numbers.

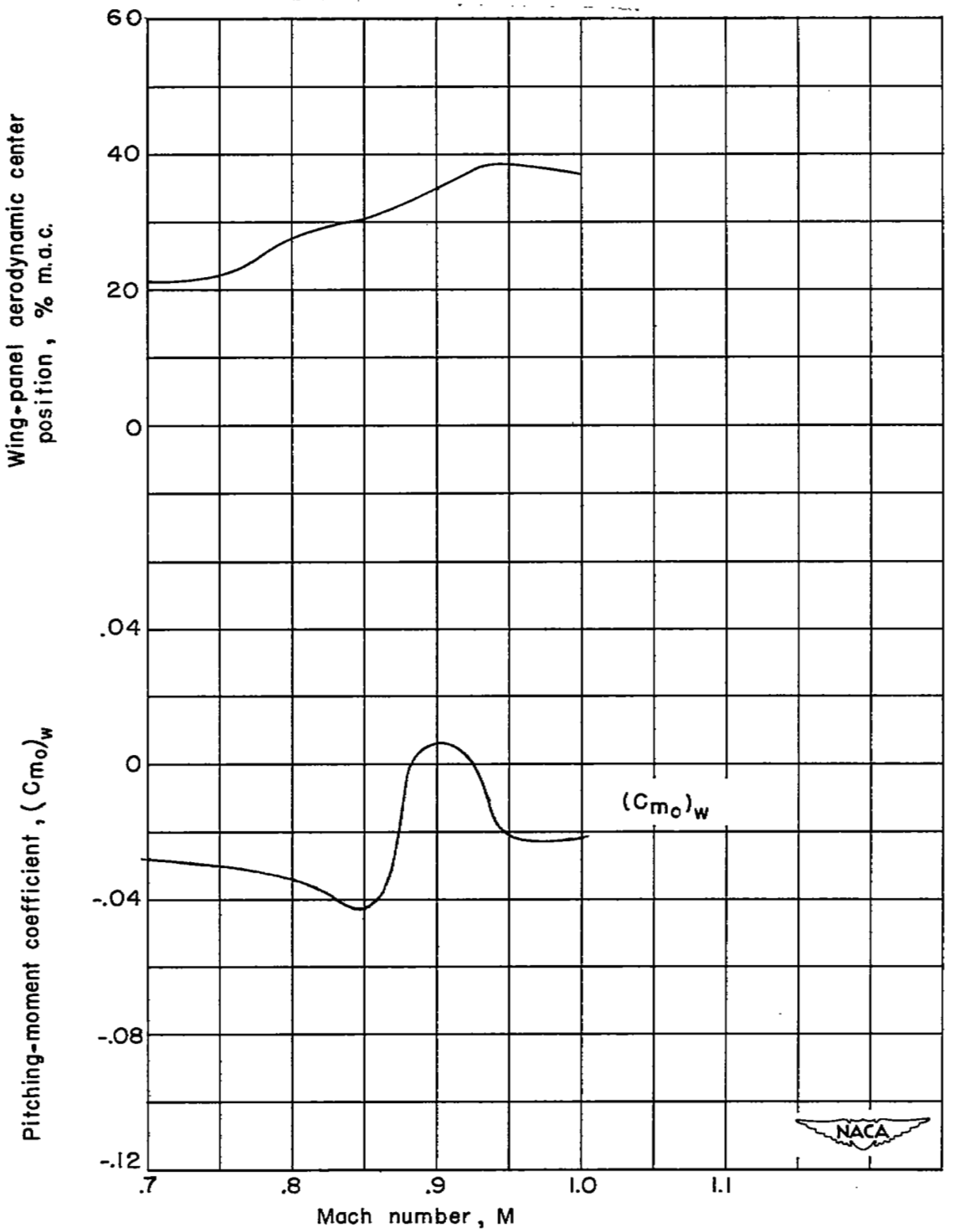

Figure 13.- Variation with Mach number of the aerodynamic-center position and the pitching moment of the wing panel at zero lift.

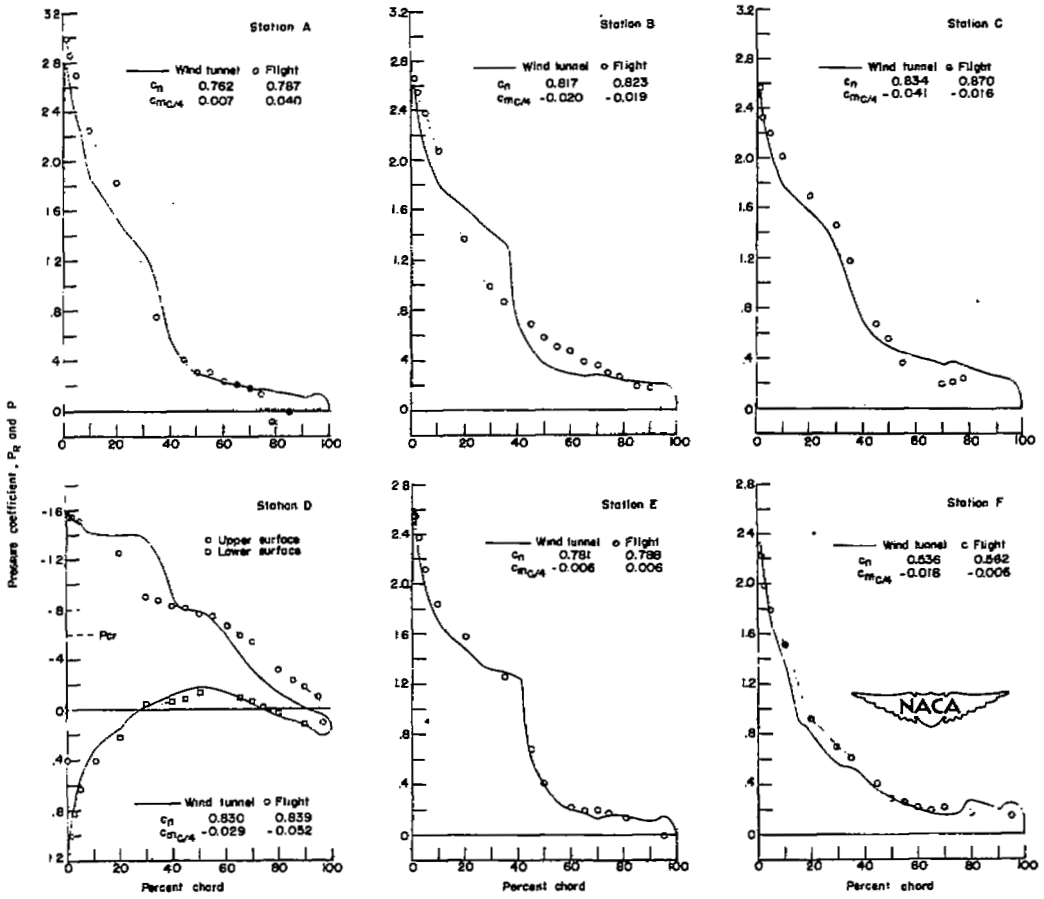

(a) Tunnel $M = 0.745$; $\alpha = 5.0^\circ$; $C_N = 0.781$. Flight data from reference 3; table 4(e); $M = 0.747$; $C_N = 0.792$; $\delta_{a_L} = 0.55^\circ$ down.

Figure 14.- Chordwise loadings and midspan pressure distributions obtained in the wind tunnel compared with flight data.

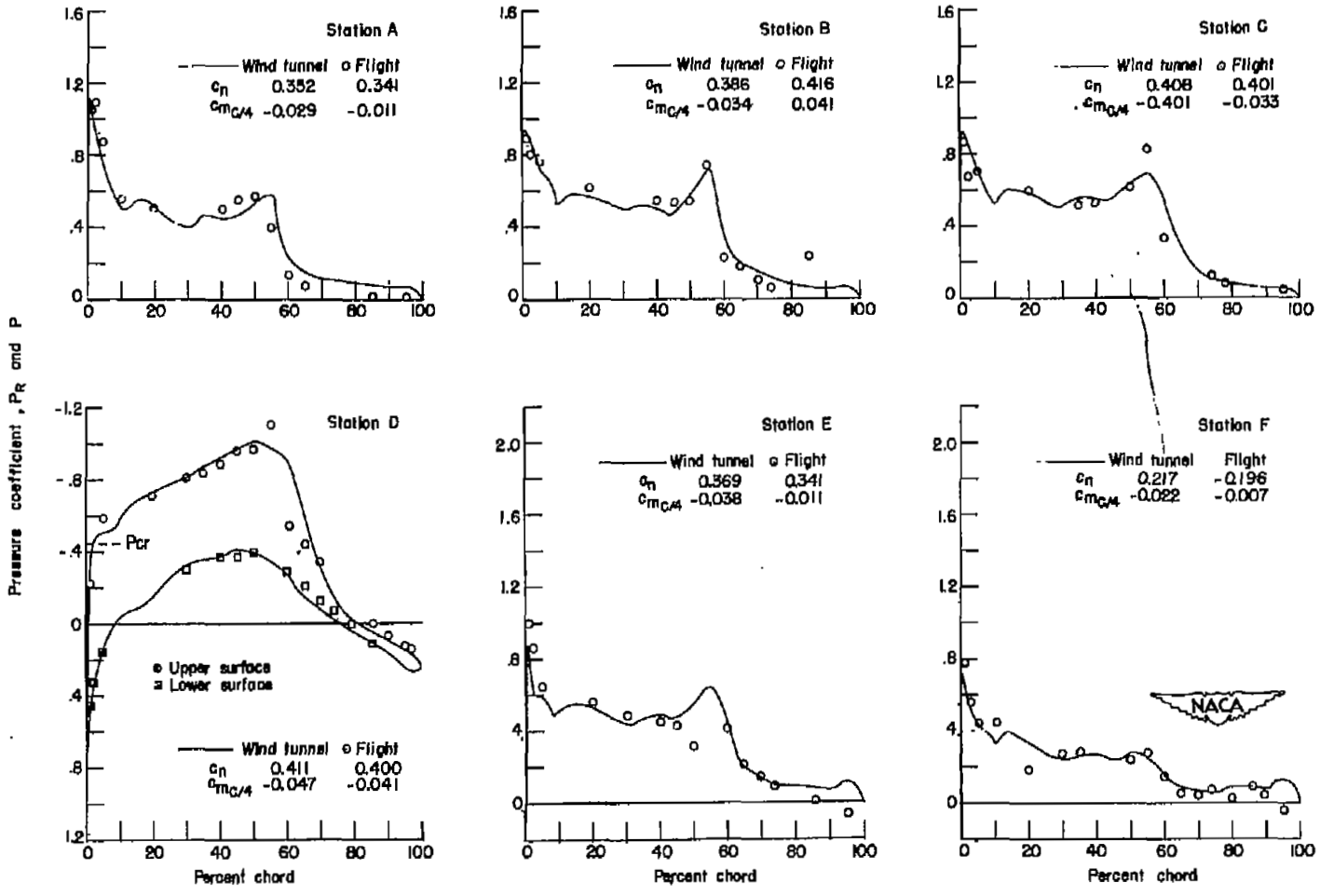

(b) Tunnel M = 0.793; $\alpha = 0.5^\circ$; $C_N = 0.369$. Flight data from reference 4; table 2(b); M = 0.808; $C_N = 0.367$; $\delta_{a_L} = 0^\circ$.

Figure 14.- Continued.

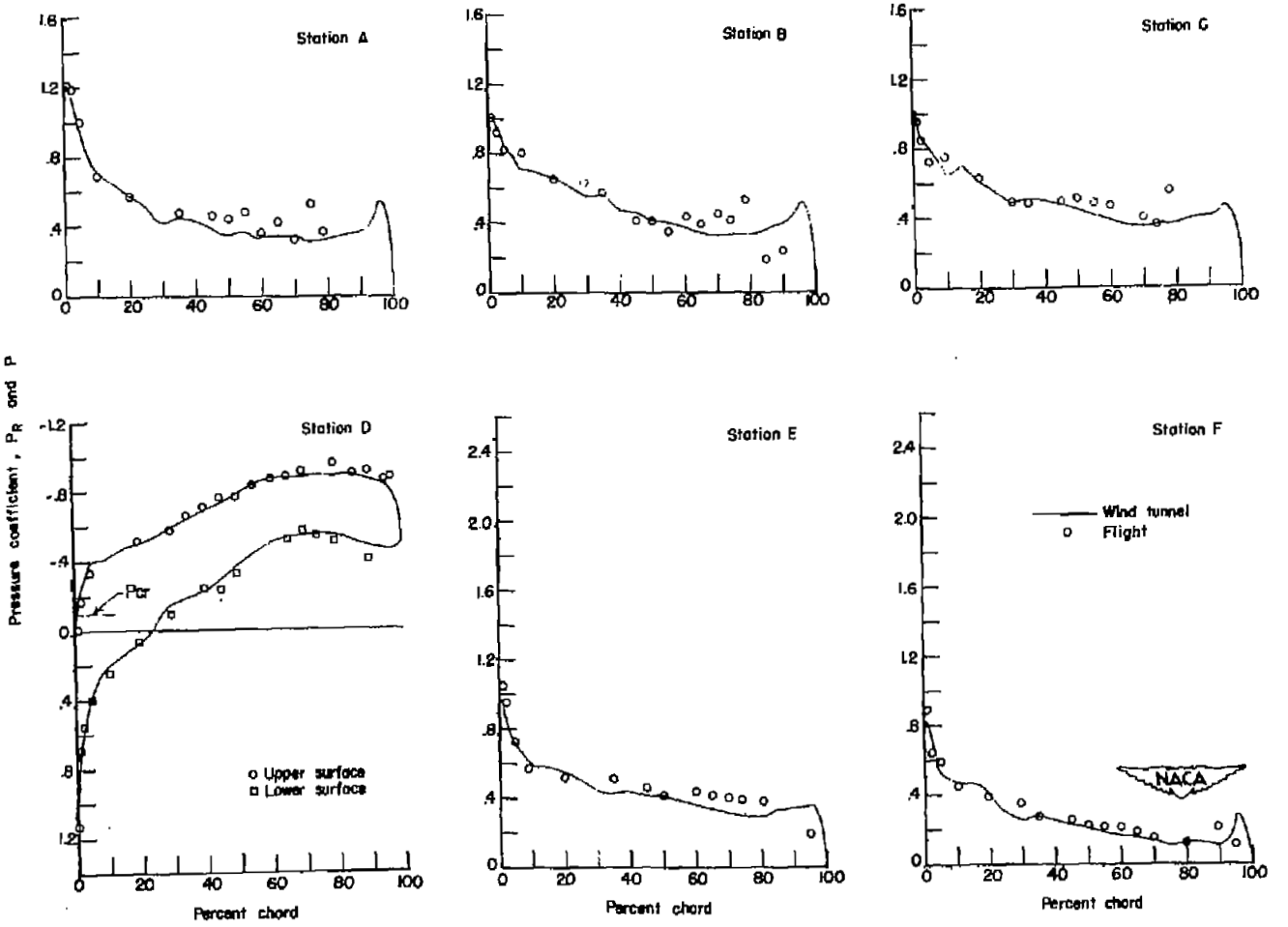

(c) Tunnel cross-plot data at M = 0.942; C_N = 0.456. Flight data from reference 3; table 6(b); M = 0.949; C_N = 0.456; δa_L = 0.80° down.

Figure 14.- Continued.

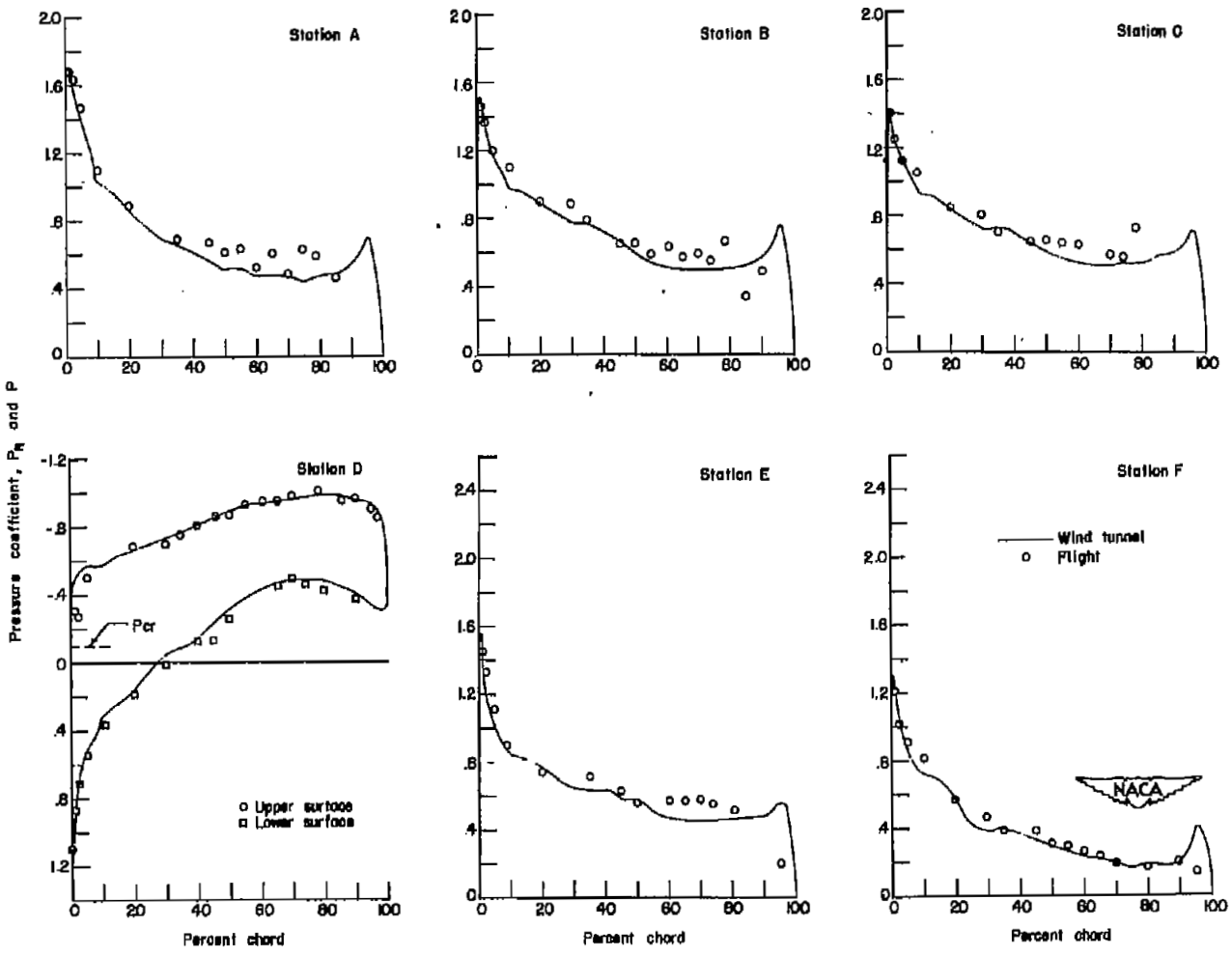

(d) Tunnel cross-plot data at $M = 0.942$; $C_N = 0.651$. Flight data from reference 3; table 6(e); $M = 0.951$; $C_N = 0.651$; $\delta_{a_L} = 0.20^\circ$ down.

Figure 14.- Continued.

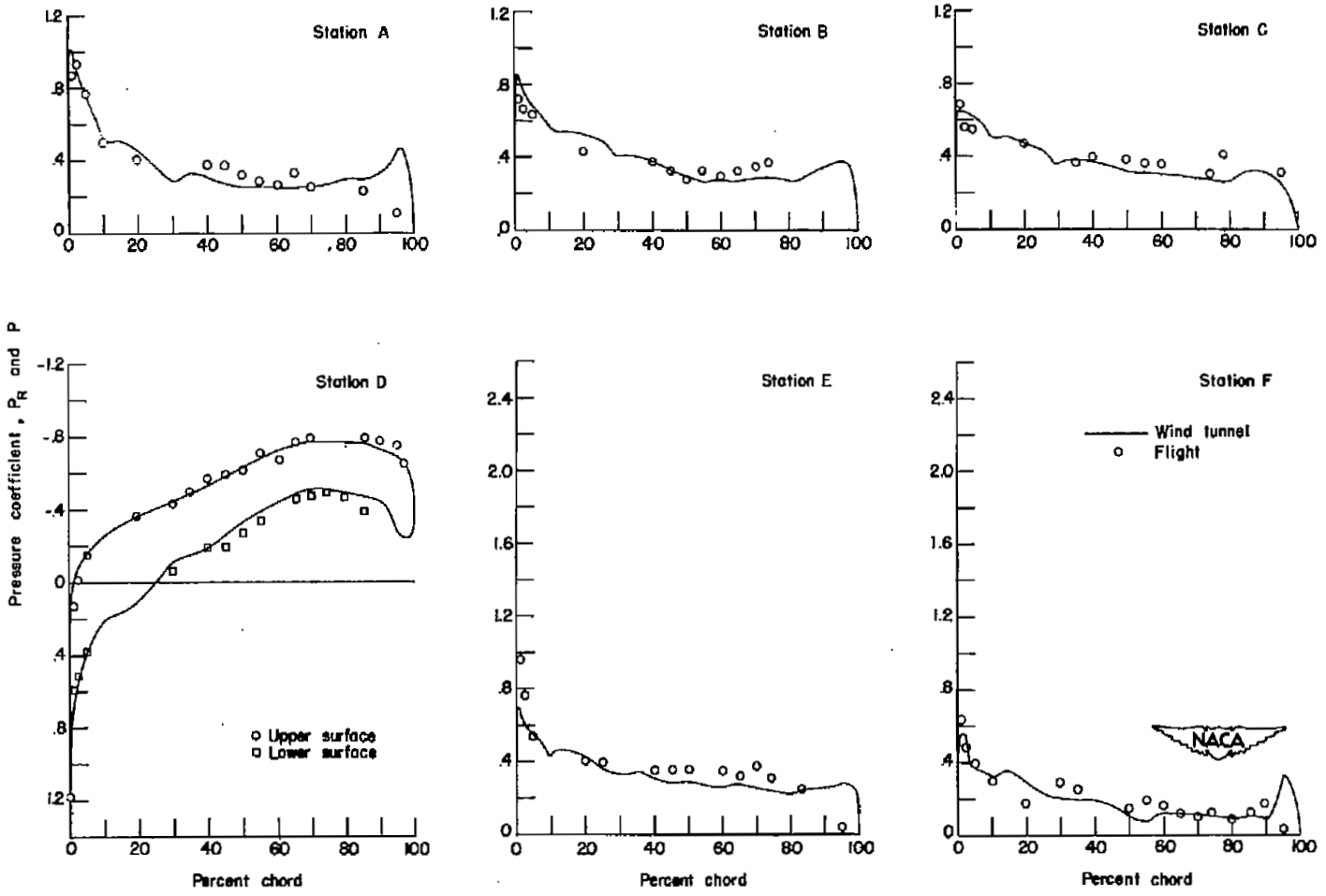

(e) Tunnel cross-plot data at M = 1.00; C_N = 0.351. Flight data from reference 4; table 2(m); M = 1.00; C_N = 0.351; δ_{a_L} = 0.89° down.

Figure 14.- Continued.

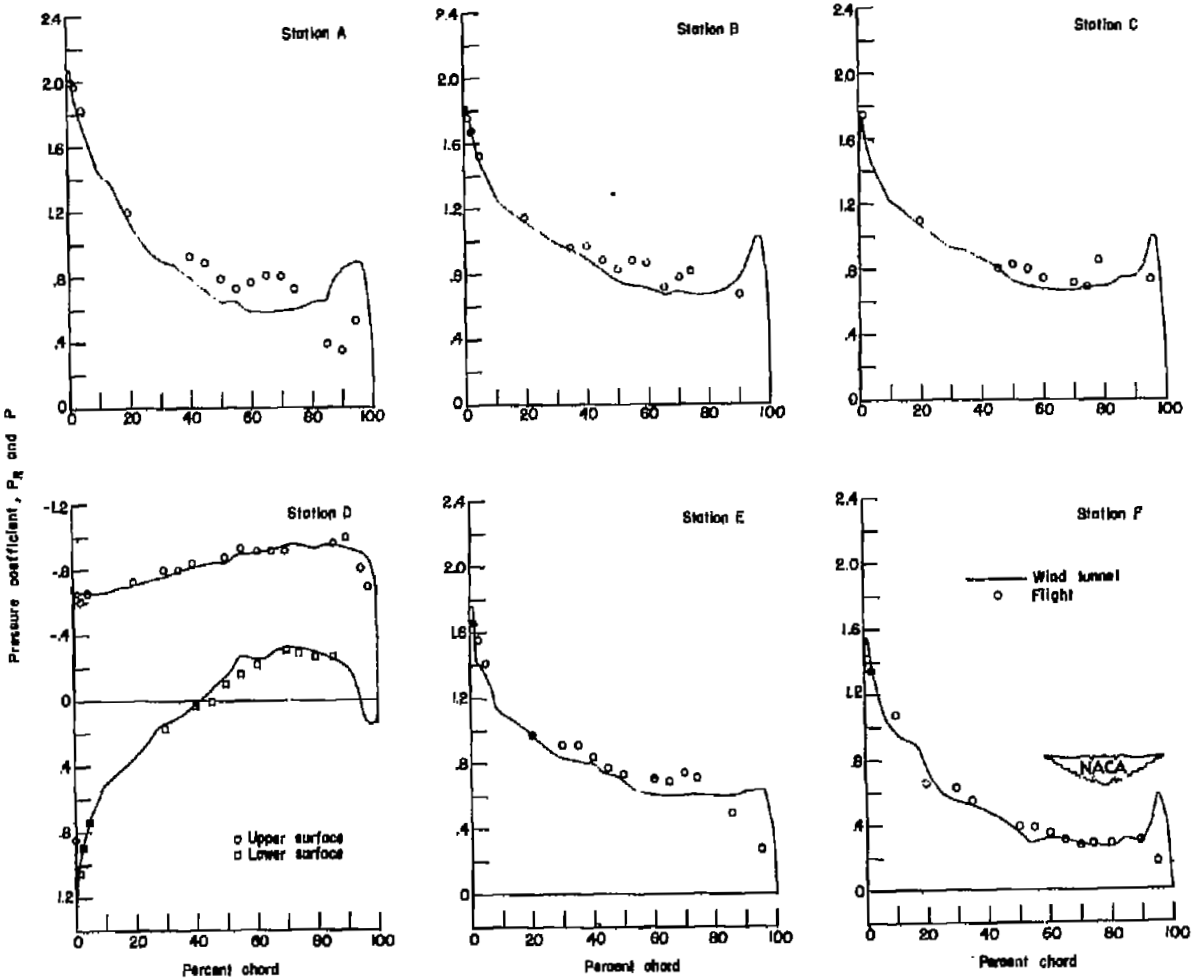

(f) Tunnel cross-plot data at M = 0.990; C_N = 0.830. Flight data from reference 5; table 11(f); M = 0.998; C_N = 0.830; δ_{a_L} = 0.61° down.

Figure 14.- Concluded.

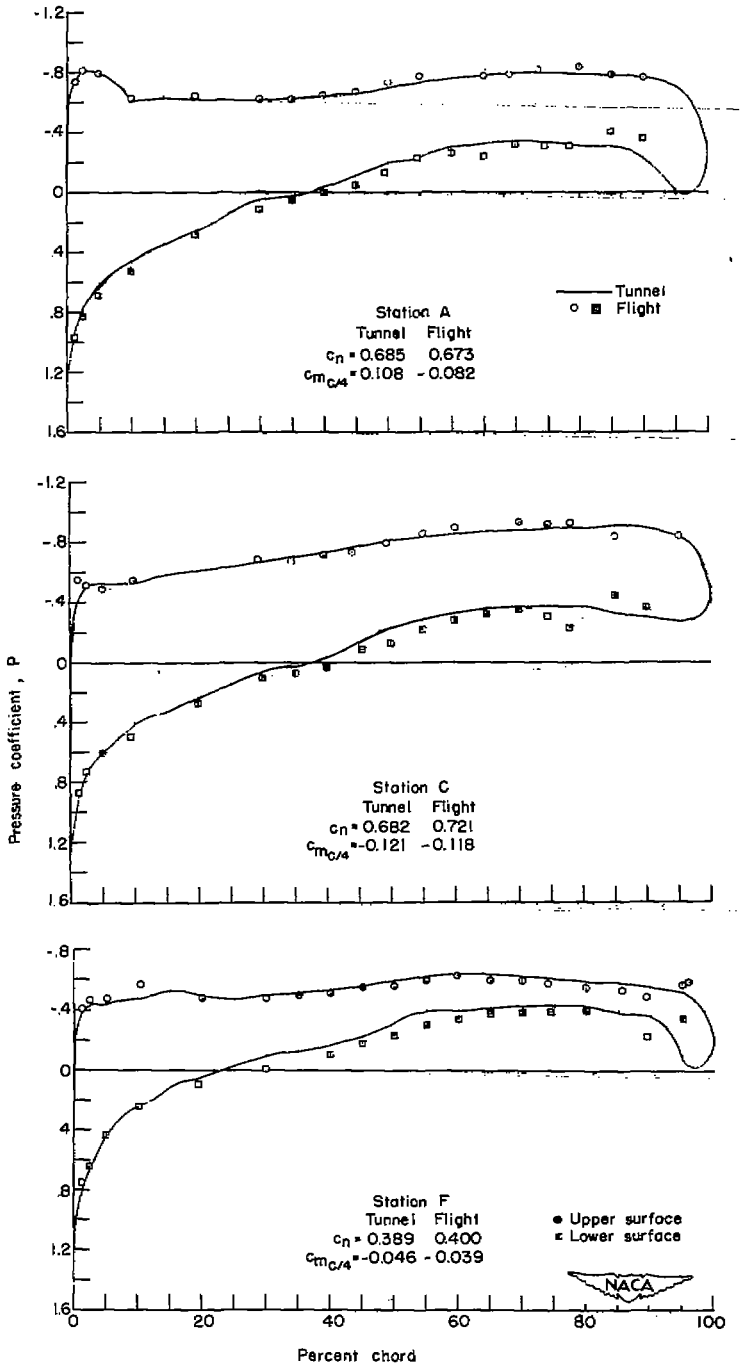

(a) Tunnel data at M = 0.986; $\alpha = 5.0^\circ$; $C_N = 0.637$; flight data at M = 0.998; $C_{N_A} = 0.593$.

Figure 15.- Chordwise pressure distribution over three spanwise wing stations obtained in the tunnel compared with flight data at speeds near Mach number 1.0.

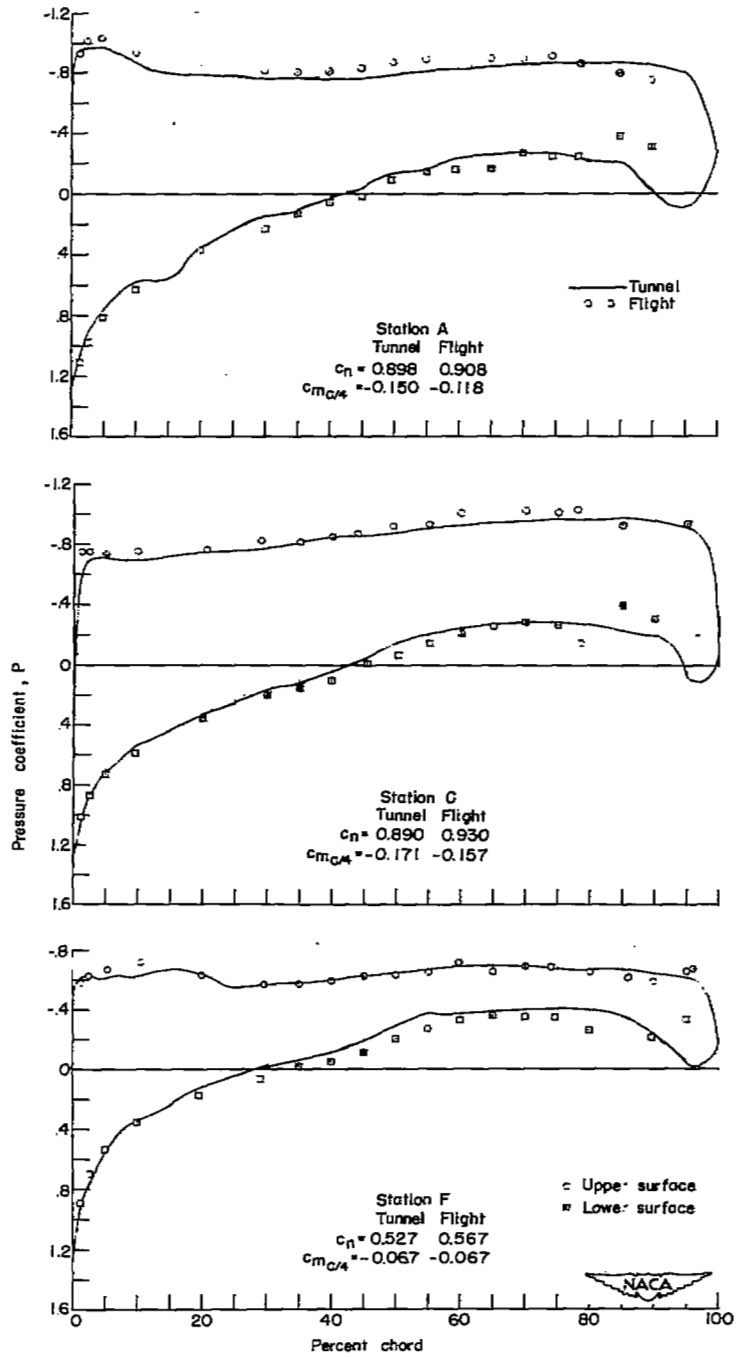

(b) Tunnel data at M = 0.988; $\alpha = 7.3^{\circ}$; $C_N = 0.834$; flight data at M = 0.991; $C_{N_A} = 0.788$.

Figure 15.- Concluded.

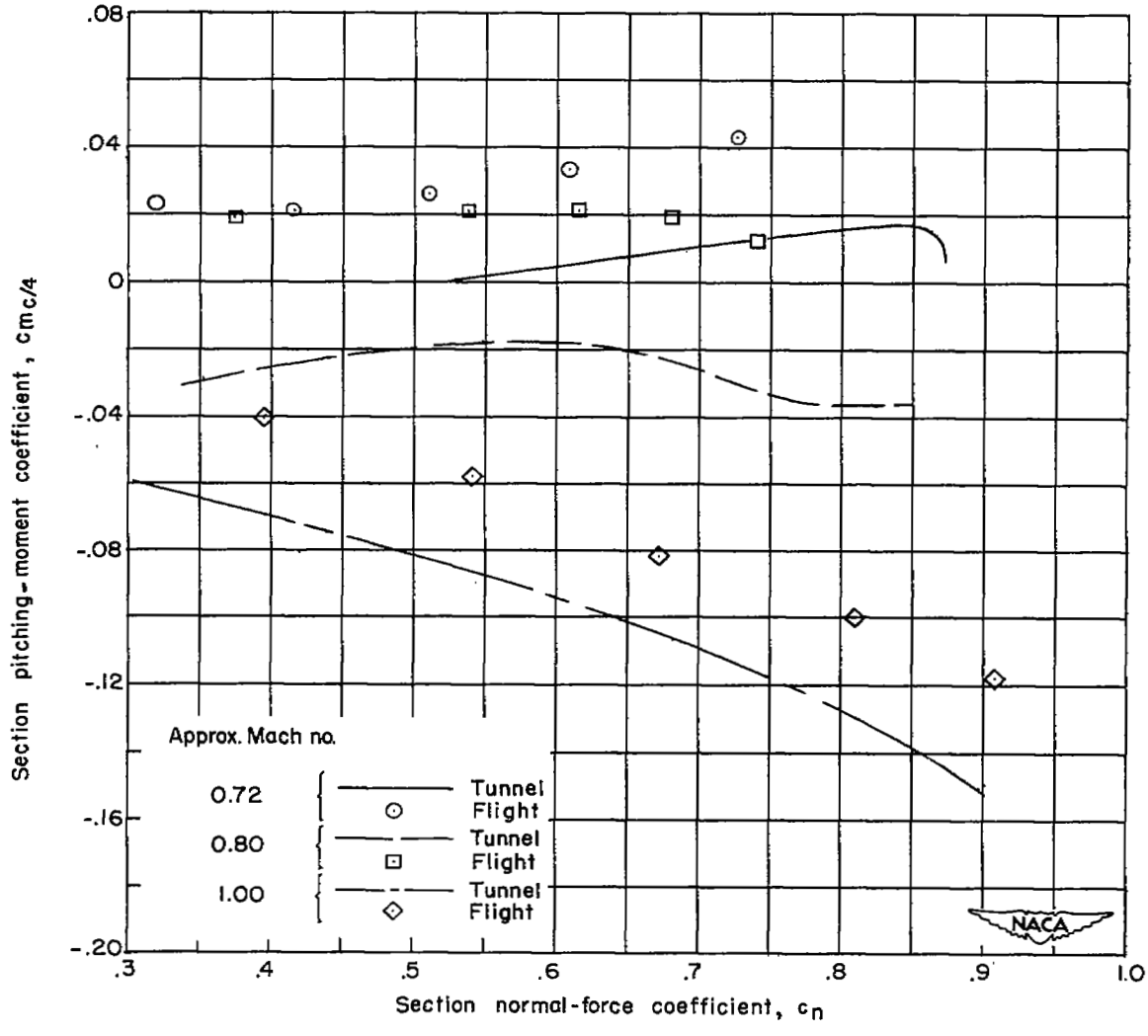

(a) Wing station A.

Figure 16.- Variation of section pitching-moment coefficient about the quarter-chord point with section normal-force coefficient.

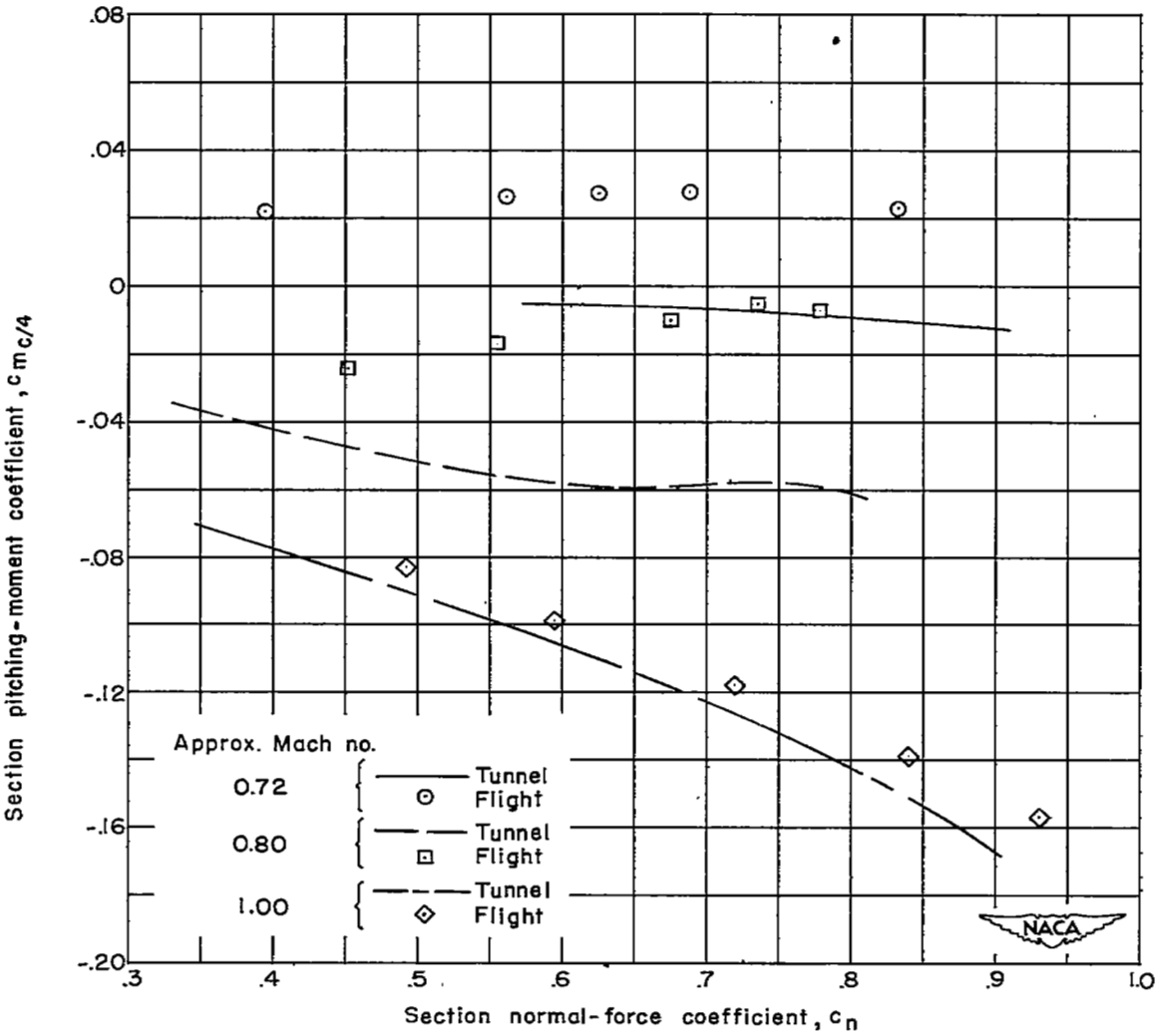

(b) Wing station C.

Figure 16.- Continued.

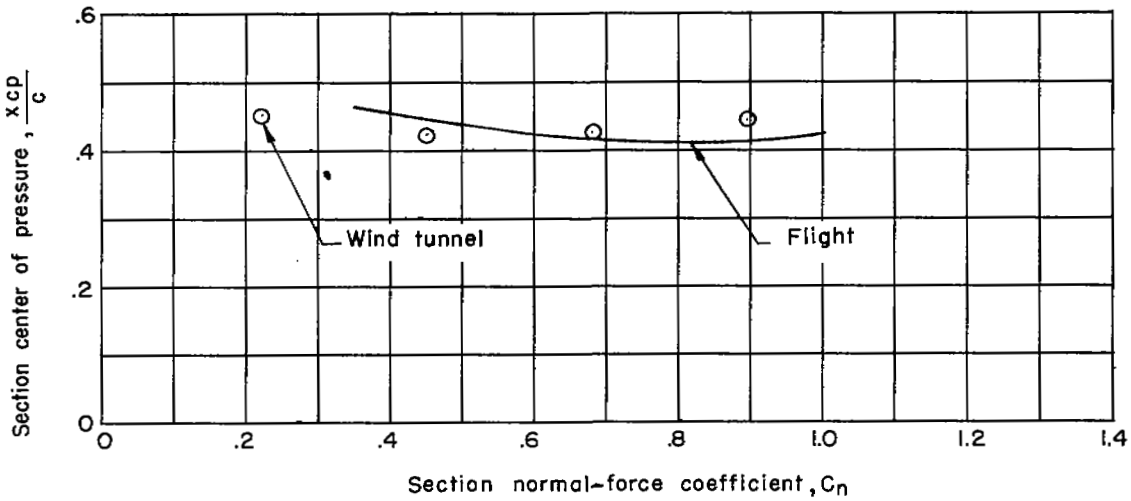

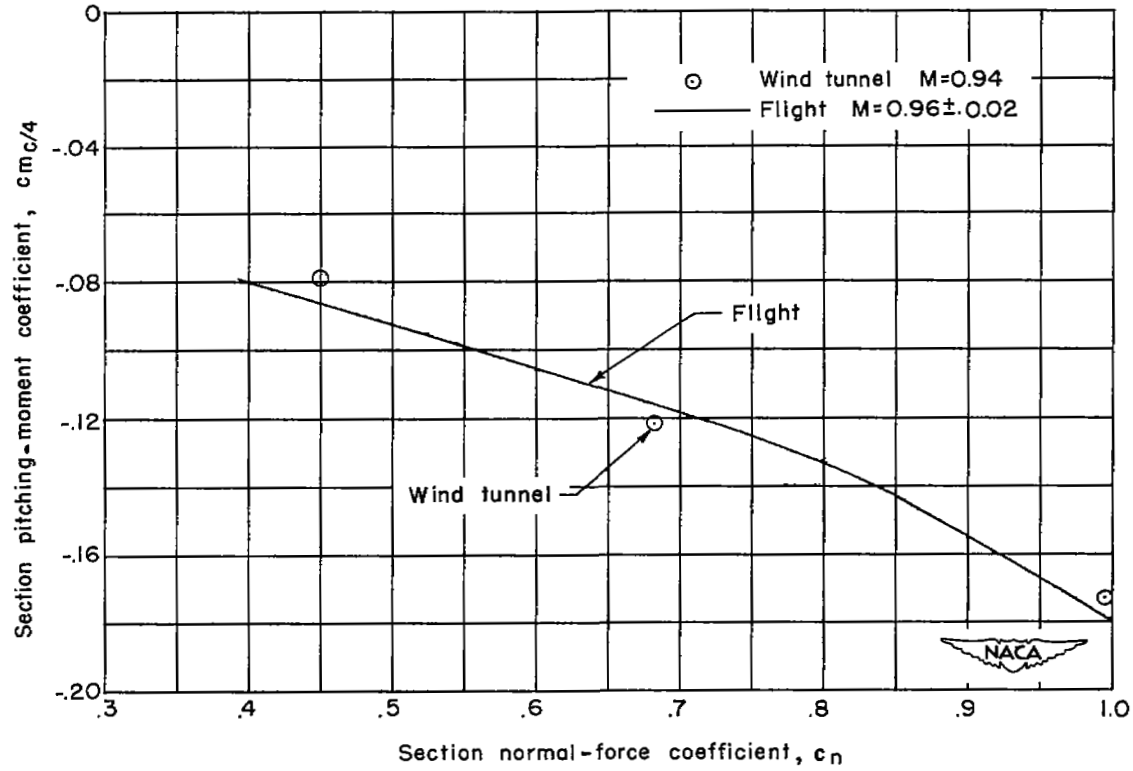

(c) Wing station D and variation of center of pressure with section normal-force coefficient.

Figure 16.- Continued.

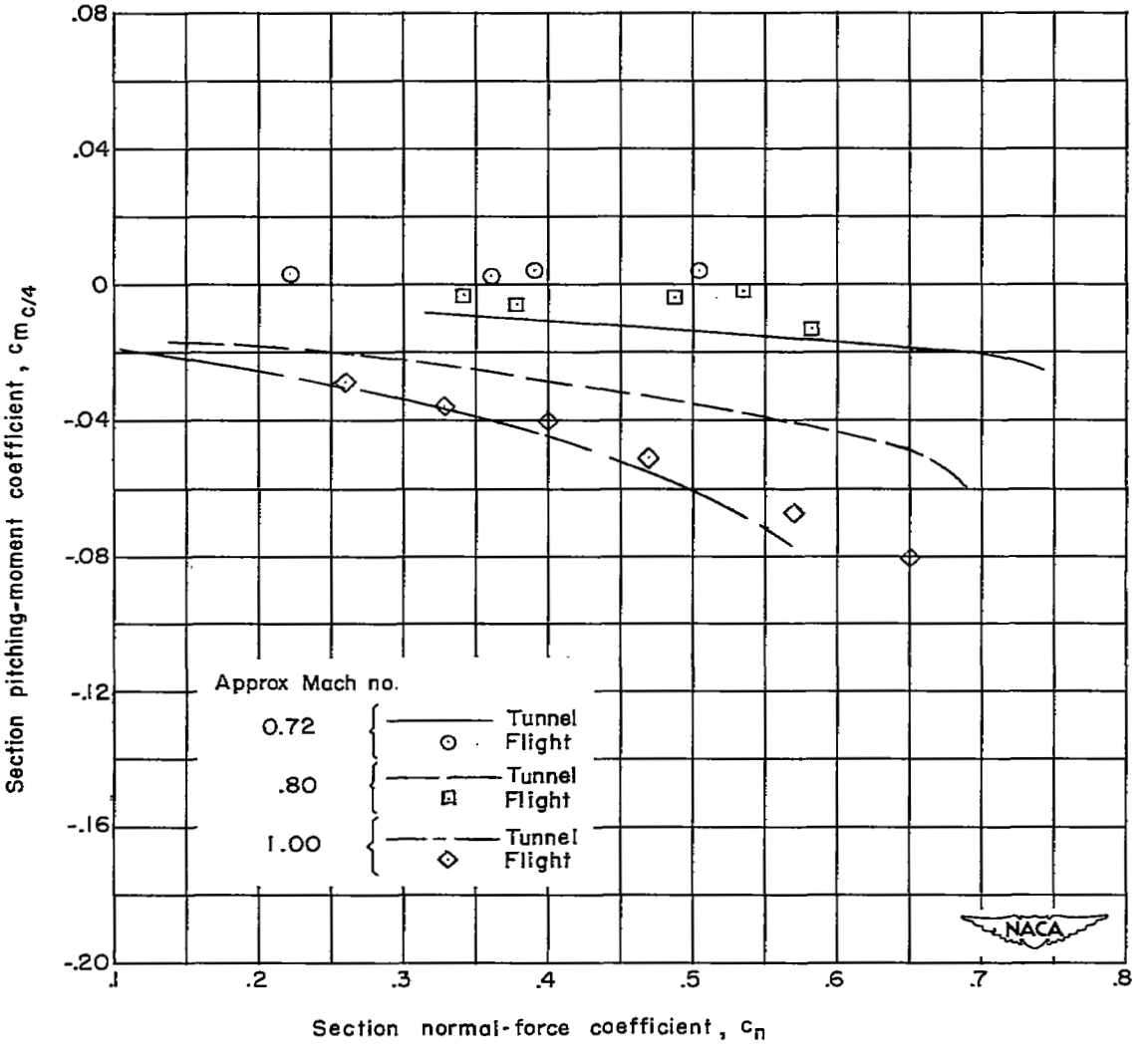

(d) Wing station F.

Figure 16.- Concluded.

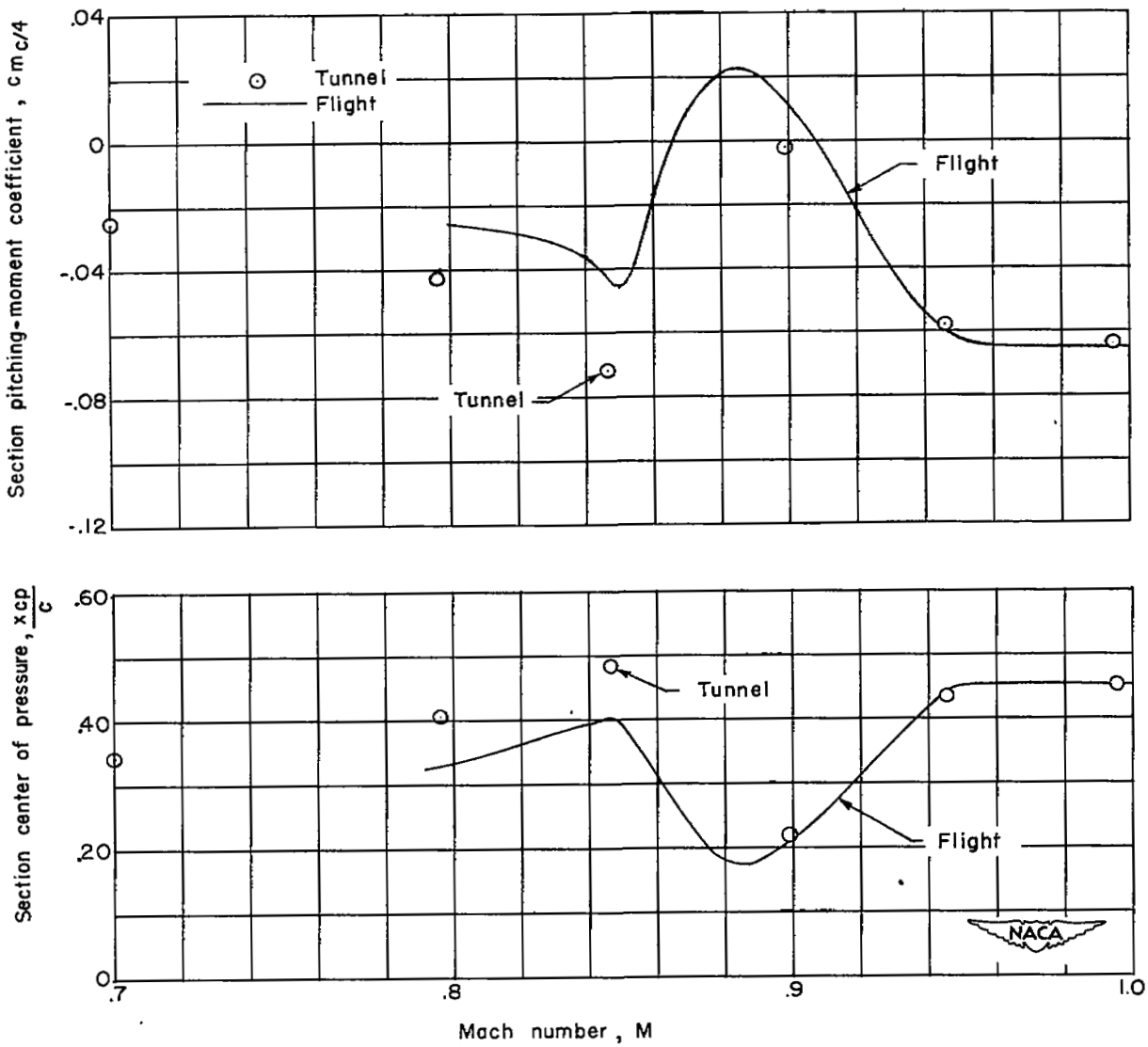

Figure 17.- Variation of section center of pressure and section pitching-moment coefficient with Mach number for wing station D. $c_n \approx 0.32$; flight data from reference 1.

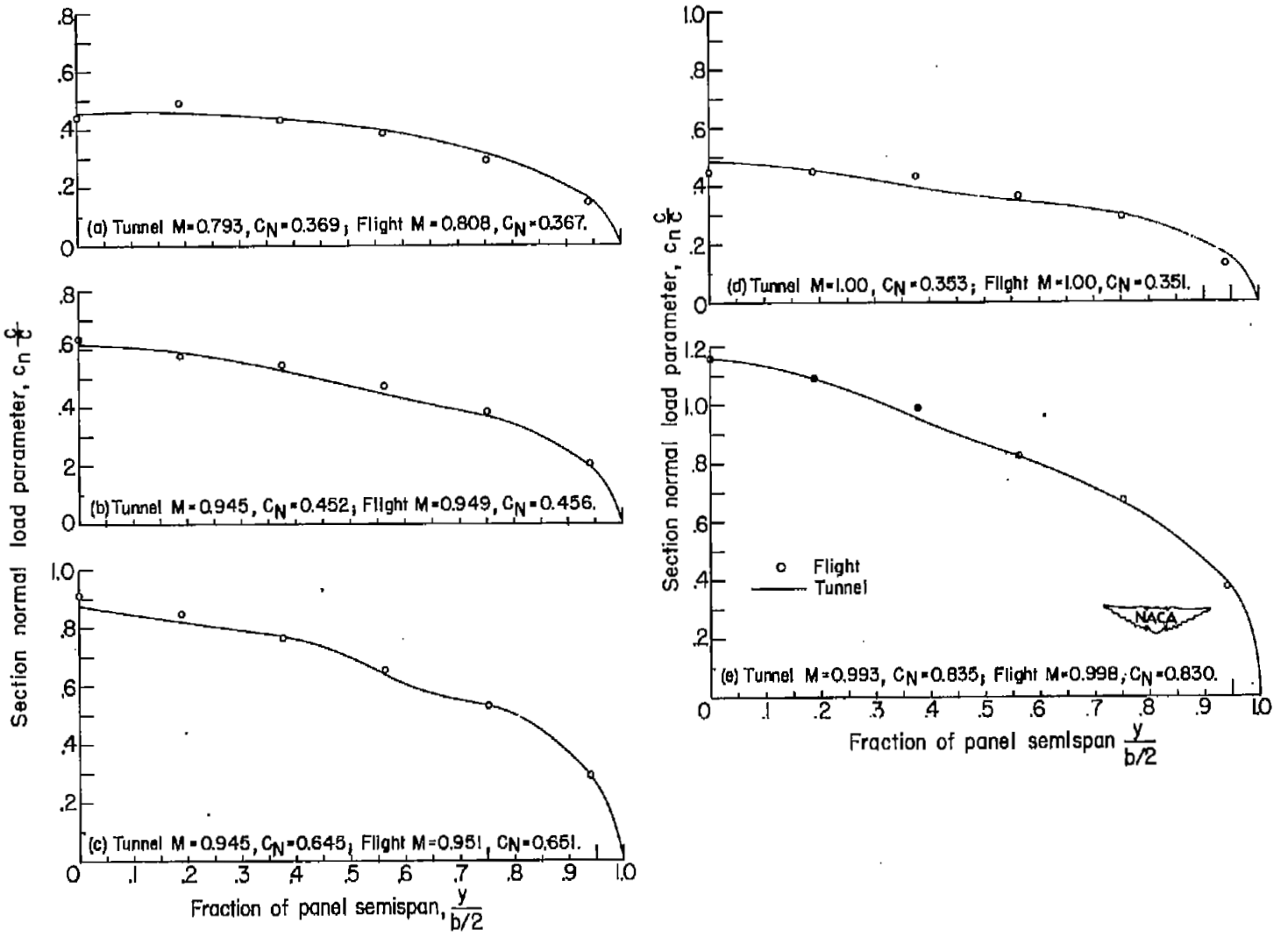

Figure 18.- Spanwise loading distributions obtained in wind tunnel and in flight at several Mach numbers.

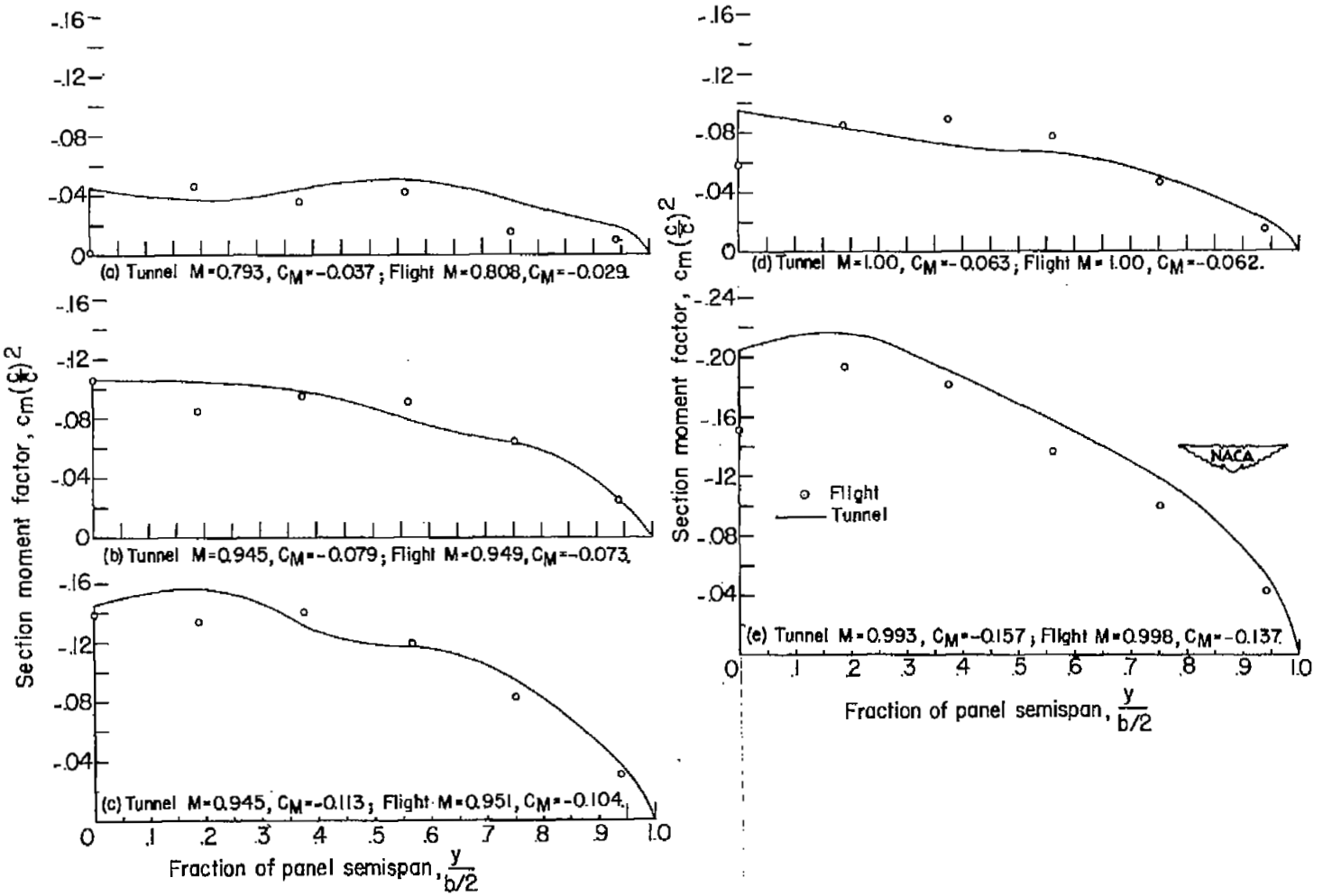

Figure 19.- Spanwise section pitching-moment distributions obtained from wind-tunnel and flight tests at several Mach numbers.

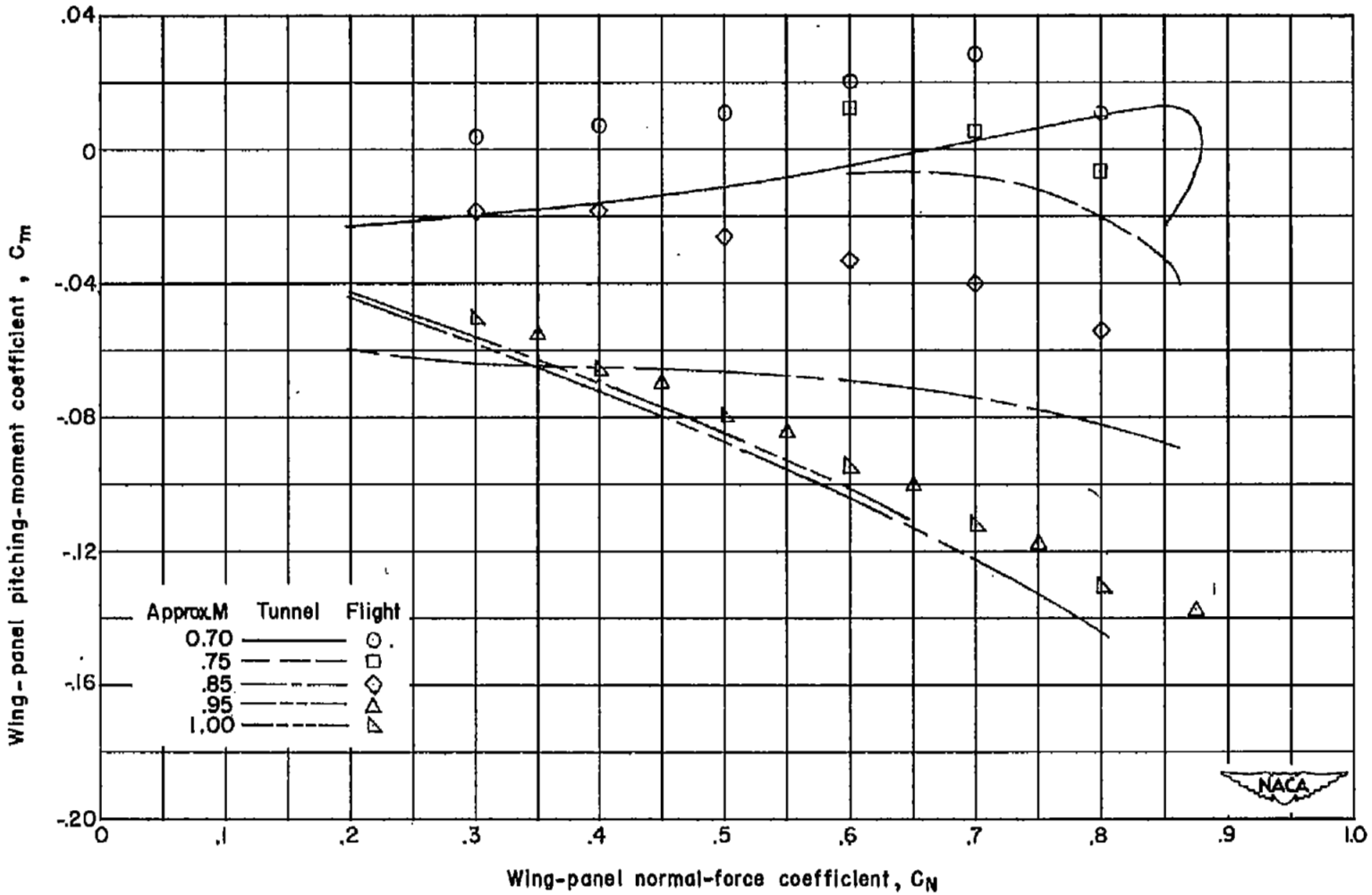

Figure 20.- Wing-panel pitching-moment coefficient about the 0.25 mean aerodynamic chord against wing-panel normal-force coefficient obtained from wind-tunnel and flight results.

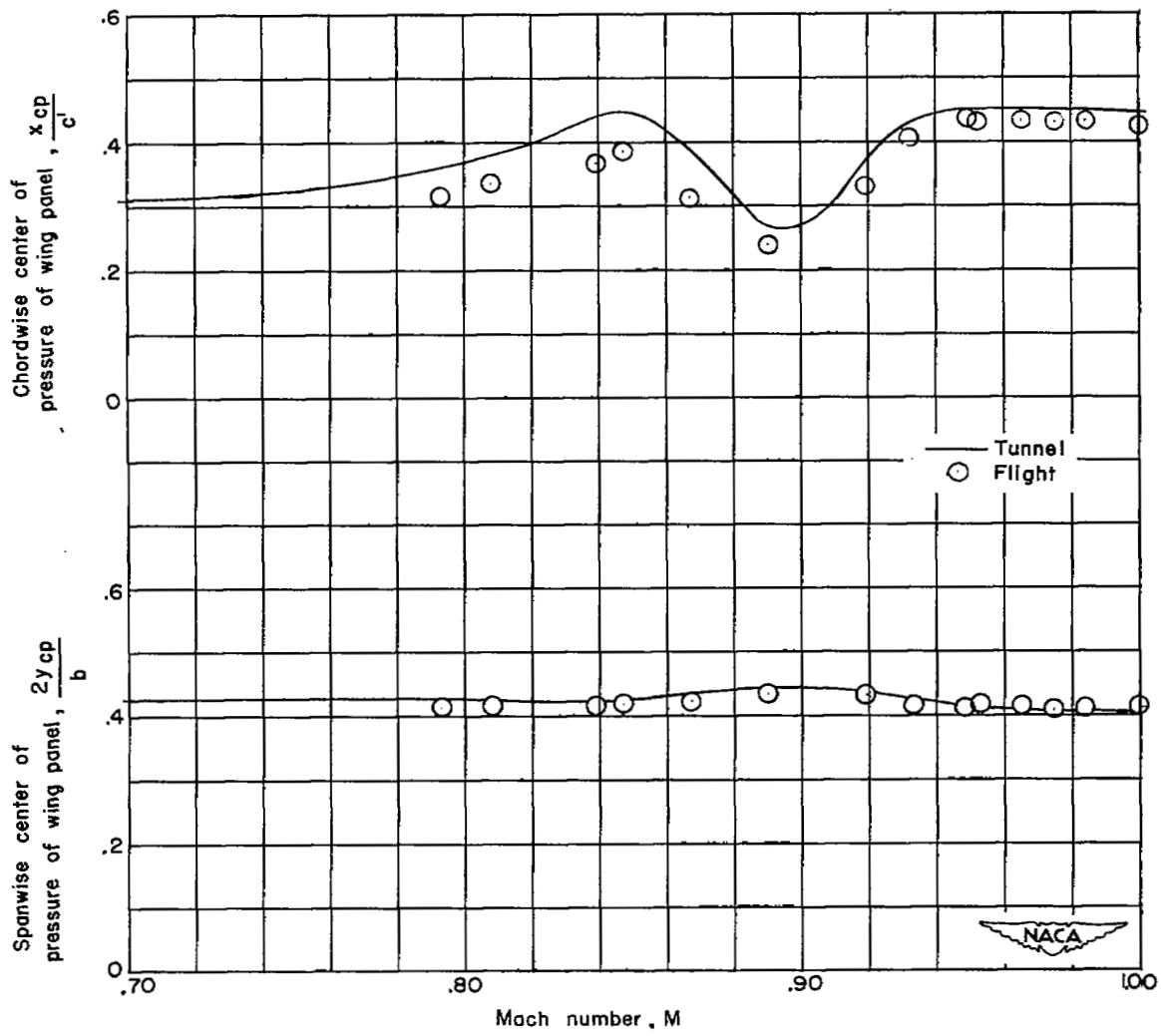

Figure 21.- Variation of chordwise and spanwise center of pressure of wing panel with Mach number obtained from wind tunnel and flight tests. $C_N = 0.35$.

NACA-Langley - 9-3-52 - 500

NASA Technical Library
3 1176 01436 4765